

UNIVERSITY OF READING
SCHOOL OF MATHEMATICS, METEOROLOGY & PHYSICS

FORWARD AND INVERSE WATER-WAVE
SCATTERING BY TOPOGRAPHY

by
CHRISTOPHER R WARNER

August 2008

This dissertation is submitted to the Department of Mathematics in partial fulfilment
of the requirements for the degree of Master of Science

Abstract

As a plane water-wave passes over a fixed underlying bed topography it scatters and a reflected wave is created travelling in the opposite direction. With knowledge of the incident wave and underlying bed topography, the reflected wave can be calculated; this is known as *forward scattering*.

Taking this reflected data we have formulated the *inverse scattering* problem, whereby we use this data in an iterative process working backwards in an effort to approximate the bed topography. This has been done using both a shallow water, and mild-slope hypothesis.

It is found that the mild-slope approximation is more accurate and reliable than the shallow water approximation at estimating the bed profile. Moreover, it is shown that with a small range of reflected data, $R(\nu)$, and some prior knowledge that the bed profile is mild, the iterative inverse method with the mild-slope approximation is able to produce an accurate representation of the underlying topography.

Acknowledgments

On the administrative side of things I would like to thank EPSRC for their financial support of the Master programme 2007-2008, and Sue Davis for all her help and guidance throughout the year. On the mathematical side I would like to thank all the lecturers for this year with particular reference to Nick Biggs and Pete Chamberlain who help me a great deal through this project, cheers guys.

Finally I have to acknowledge all the people in 105 and thank them for a great year, a busy year but a great year nonetheless. And a special mention to the main motivational tool of the year - the 'I Don't Care!' sign.

Declaration

I confirm that this is my own work and the use of all material from other sources has been properly and fully acknowledged.

Signed..... Date.....

Contents

Abstract	ii
1 Introduction	1
2 Linear Wave Scattering by Topography	4
2.1 Equations of Velocity Potential	4
2.1.1 Reflection and Transmission Coefficients	6
2.2 Approximations of the Equations	7
2.2.1 Variational Approximation	7
2.2.2 Shallow Water and Mild-Slope Approximations	8
3 Forward Wave Scattering	11
3.1 Shallow Water Approximation	12
3.1.1 Formulating the Problem	13
3.1.2 Difficulties For Large ν	14
3.2 Mild-Slope Approximation	15
3.2.1 Formulating the Problem	16
3.2.2 The Behaviour of R	17
3.3 Implementation	19

3.4	Extensions	20
4	Inverse Wave Scattering	22
4.1	Shallow Water Approximation	23
4.1.1	A First Approximation - $h_1(t)$	23
4.1.2	Further Approximations - $h_{n+1}(t)$	25
4.2	Mild-Slope Approximation	27
4.2.1	A First Approximation - $h_1(t)$	27
4.2.2	Further Approximations - $h_{n+1}(t)$	29
4.3	Implementation	30
4.4	A Possible Extension	32
5	Results	35
5.1	Accuracy of First Approximations $h_1(x)$	37
5.1.1	Shallow Water Approximation	37
5.1.2	Mild-Slope Approximation	39
5.2	Convergence of Iterations	40
5.2.1	Shallow Water Approximation	41
5.2.2	Mild-Slope Approximation	45
5.3	Further Testing	50
5.3.1	Greater Accuracy?	51
5.3.2	Sensitivity to Changes in (ν_1, ν_2)	52
5.3.3	The Affect of Amplitude	55
6	Summary, Future Work & Conclusions	57
	Bibliography	61

CONTENTS vi

A More Tables And Figures **62**

 A.1 Shallow Water Approximation 62

 A.2 Mild-Slope Approximation 66

List of Figures

3.1	Graphical representation of the forward scattering problem, where R and T are the reflection and transmission amplitudes respectively and $h(x)$ is the quiescent depth.	11
3.2	Plot of $ R(\nu) $ using the shallow water approximation, where $l = 5$ and $h(x) = 0.2 - 0.05 \times \sin(2\pi x/5)$	14
3.3	Plot of $ R(\nu) $ using the mild-slope approximation, where $l = 5$ and $h(x) = 0.2 - 0.05 \times \sin(2\pi x/5)$	17
3.4	Plots of $ R(\nu) $, where $l = 5$ and $h(x) = 0.2 - 0.05 \times \sin(2\pi x/5)$ with $M = 100$ and $M = 1000$ respectively	20
4.1	Graphical representation of the inverse scattering problem, where R and T are the reflection and transmission amplitudes respectively and $h(x)$, the quiescent depth, is to be found.	22
4.2	$h_1(t)$ (green) as found by (4.5) and (4.6) respectively to approximate bed topography (brown).	25
5.1	Depth profile $h_A(x)$	35
5.2	Depth profile $h_B(x)$	36
5.3	Depth profile $h_C(x)$	36
5.4	Comparison of h_1 with h_2 using $h = h_B$ and $\nu_2 = 1$	42
5.5	Converged depth profiles for h_A , h_B and h_C respectively with $\nu_2 = 0.3$, using the shallow water approximation.	45

5.6	Comparison of h_1 with h_2 using $h = h_B$ and $\nu_2 = 1$.	47
5.7	Converged depth profiles for h_A , h_B and h_C respectively with $\nu_2 = 1$, using the mild-slope approximation.	50
5.8	$ R(\nu) $ for $h = h_A$ and $h = h_C$ respectively.	51
5.9	Converged depth profiles for $h = h_A$ using the mild-slope approximation, where ν_2 has been allowed to vary.	52
5.10	Converged depth profiles for $h = h_B$ using the mild-slope approximation, where ν_2 has been allowed to vary.	53
5.11	Converged depth profiles for $h = h_C$ using the mild-slope approximation, where ν_2 has been allowed to vary.	53
5.12	Converged depth profiles for $h = h_A$ using the mild-slope approximation, where ν_1 has been allowed to vary.	54
5.13	Converged depth profiles for $h = h_B$ using the mild-slope approximation, where ν_1 has been allowed to vary.	54
5.14	Converged depth profiles for $h = h_C$ using the mild-slope approximation, where ν_1 has been allowed to vary.	55
5.15	Depth profile $h = h_A$ with $\epsilon = 0.1$	56
A.1	Comparison of h_1 with h_2 using $h = h_A$ and $\nu_2 = 1$.	63
A.2	Comparison of h_1 with h_2 using $h = h_C$ and $\nu_2 = 1$.	64
A.3	Converged depth profiles for h_A , h_B and h_C respectively with $nu_2 = 0.5$, using the shallow water approximation.	64
A.4	Converged depth profiles for h_A , h_B and h_C respectively with $nu_2 = 0.7$, using the shallow water approximation.	65
A.5	Comparison of h_1 with h_2 using $h = h_A$ and $\nu_2 = 1$.	67
A.6	Comparison of h_1 with h_2 using $h = h_C$ and $\nu_2 = 1$.	67
A.7	Converged depth profiles for h_A , h_B and h_C respectively with $\nu_2 = 5$, using the mild-slope approximation.	68

A.8 Converged depth profiles for h_A , h_B and h_C respectively with $\nu_2 = 15$, using the mild-slope approximation. 68

List of Tables

5.1	Error analysis of $h_1(x)$ as an approximation to $h(x)$ using the shallow water approximation.	38
5.2	Error analysis of $h_1(x)$ as an approximation to $h(x)$ using the mild-slope approximation.	39
5.3	Error between $(m)^{\text{th}}$ and $(m-1)^{\text{th}}$ iterate with $\nu_2 = 0.5$, using shallow water approximation.	41
5.4	Error between $(m)^{\text{th}}$ and $(m-1)^{\text{th}}$ iterate with $\nu_2 = 1$, using shallow water approximation.	41
5.5	Comparing the relative error of $h_1(x)$ with $h_2(x)$	42
5.6	Comparing the total error of $h_1(x)$ with $h_2(x)$	42
5.7	Error between $(n)^{\text{th}}$ and $(n-1)^{\text{th}}$ iterate using the shallow water approximation.	43
5.8	Error analysis of $h_n(x)$ to $h(x)$ using the shallow water approximation.	44
5.9	Error between $(m)^{\text{th}}$ and $(m-1)^{\text{th}}$ iterate with $\nu_2 = 0.5$, using mild-slope approximation.	46
5.10	Error between $(m)^{\text{th}}$ and $(m-1)^{\text{th}}$ iterate with $\nu_2 = 1$, using mild-slope approximation.	46
5.11	Error between $(m)^{\text{th}}$ and $(m-1)^{\text{th}}$ iterate with $\nu_2 = 10$, using mild-slope approximation.	46
5.12	Comparing the relative error of $h_1(x)$ with $h_2(x)$	47
5.13	Comparing the total error of $h_1(x)$ with $h_2(x)$	47
5.14	Error between $(n)^{\text{th}}$ and $(n-1)^{\text{th}}$ iterate using mild-slope approximation.	48
5.15	Error analysis of $h_n(x)$ to $h(x)$ using the mild-slope approximation.	49

5.16 Relative error of converged approximation, $h_n(x)$ to $h(x)$, using the mild-slope approximation and a fixed $\Delta\nu$ 51

A.1 Maximum error between the $(m)^{th}$ and $(m-1)^{th}$ iterate with $\nu_2 = 5$, using the shallow water approximation. 62

A.2 Maximum error between the $(m)^{th}$ and $(m-1)^{th}$ iterate with $\nu_2 = 10$, using the shallow water approximation. 63

A.3 Maximum error between the $(m)^{th}$ and $(m-1)^{th}$ iterate with $\nu_2 = 15$, using the shallow water approximation. 63

A.4 Maximum error between the $(m)^{th}$ and $(m-1)^{th}$ iterate with $\nu_2 = 5$, using the mild-slope approximation. 66

A.5 Maximum error between the $(m)^{th}$ and $(m-1)^{th}$ iterate with $\nu_2 = 15$, using the mild-slope approximation. 66

Chapter 1

Introduction

As a plane water-wave passes over a fixed underlying bed topography, part of the incident wave is reflected back and some is transmitted forward. This process is referred to as *wave scattering*.

Linear Wave Scattering by Topography

The governing equations are based on the fluid dynamics of the water, that is by assuming irrotation flow and using linearised boundary conditions for both the free surface and underlying topography, where we are concerned with motion in the (x, z) plane and consider the bed profile $h = h(x)$. Here z is chosen to point vertically upwards and x is a horizontal variable. This approach leads to a boundary value problem for the velocity potential, which has been solved using separation of variables and from which we can derive radiation conditions (the behaviour as $|x| \rightarrow \infty$). From these radiation conditions, reflection and transmission coefficients, R_{\pm} and T_{\pm} respectively, can be defined.

To simplify the boundary value problem an approximation to the solution can be used, and in our case we shall use both the shallow water and mild-slope approximations. The shallow water approximation is based on the hypothesis that the wavelength is much greater than the quiescent depth, and the mild-slope approximation is based on the idea that $h'(x) \ll 1$, where prime denotes differentiations with respect to x .

Forward Wave Scattering

The *forward wave scattering* problem is concerned with finding the amplitude of the reflected and transmitted waves given that we know the amplitude of the incident wave, for any specified wave number $\nu = \omega^2/g$, where ω is the wave frequency and g is the acceleration due to gravity. In fact only the reflected wave amplitude need be found since the reflection and transmission coefficients are connected by certain identities.

To find the reflected wave amplitude $R(\nu)$ we assume that the bed topography, $h(x)$, is known and then use the shallow water and mild-slope approximations to formulate new boundary value problems (and equivalent integral equations). With the solution to these problems and the use of an appropriate substitution, $R(\nu)$ can be evaluated explicitly. We will be investigating the behaviour of R for the different approximations, in particular what happens as $\nu \rightarrow \infty$.

Inverse Wave Scattering

The *inverse wave scattering* problem is simply working backwards through the forward scattering problem, taking the reflected wave amplitude and attempting to find the underlying topography for $x \in (0, l)$, for some $l > 0$. For this we assume that $R(\nu)$ is known for some $\nu \in (0, \infty)$ and also that the depth is known at the boundaries i.e. at $x = 0$ and $x = l$. The procedure that we then adopt is an iterative one where we use an approximation $h_n(x)$ to $h(x)$, and seek to improve this to attain a new approximation $h_{n+1}(x)$.

The method that shall be implemented involves finding approximations to the solutions of the boundary value problems, formulated for the forward scattering problem, placing these in the expression for $R(\nu)$ and inverting using Fourier transforms to attempt to find a better approximation. The iteration process is split into what we shall call ‘inner’ and ‘outer’ iterations, where the inner iteration deals with extracting a new iterate, $h_{n+1}(x)$, from $R(\nu)$ using Fourier transforms, and the outer iteration uses this new iterate to find a better approximation to the solution of the boundary value problem (or integral equations). This process is then repeated until the approximation has converged, hopefully to the true solution $h(x)$.

Testing

It is not yet known whether the iteration process for solving the inverse scattering problem, in general, converges. For this reason we shall be testing both the inner and outer iterations to see if they do in fact converge, and if so whether this limit is the desired solution.

We shall also be investigating just how much of the reflected information, $R(\nu)$, we need to be able to find a reasonable approximation since it is not practical to find $R(\nu)$ for all $\nu \in (0, \infty)$, but instead to approximate this by some range, (ν_1, ν_2) say. We will also be testing for certain limitations of the inverse problem, i.e. what type of topography can the shallow water and mild-slope approximations handle and still remain reasonably accurate.

Chapter 2

Linear Wave Scattering by Topography

Before looking into the main problem of forward and inverse wave scattering by topography we first need to review some established work on wave scattering, as we will be using this work as a foundation to what follows.

2.1 Equations of Velocity Potential

If we consider the three dimensional case with depth z , where $-h < z < 0$ and the bed profile $h = h(x, y)$, then we can formulate equations for the time-independent velocity potential $\phi(x, y, z)$. By assuming that the flow is irrotational and by using linearised boundary conditions for the free surface of the water and bed topography, we have

$$\left. \begin{aligned} \nabla^2 \phi &= 0 & (-h < z < 0) \\ \phi_z - \nu \phi &= 0 & (z = 0) \\ \phi_z + \nabla_h h \cdot \nabla_h \phi &= 0 & (z = -h) \end{aligned} \right\}, \quad (2.1)$$

where $\nabla_h = (\partial/\partial x, \partial/\partial y)$ and $\nu = \omega^2/g$ with ω being the prescribed angular wave frequency and g the acceleration due to gravity.

However we are not concerned with the full three-dimensional problem but a simpler case in which plane waves propagate parallel to the x -axis. This means we instead have $h = h(x)$ so that $\phi = \phi(x, z)$ and therefore separation of variables used on (2.1) gives

$$\phi(x, z) = (A_0 e^{ikx} + B_0 e^{-ikx}) Z_0(z, h) + \sum_{n=1}^{\infty} (A_n e^{k_n x} + B_n e^{-k_n x}) Z_n(z, h), \quad (2.2)$$

on an interval where h is constant, for some constants A_n, B_n ($n \geq 0$). Here,

$$\left. \begin{aligned} Z_0(z, h) &= c_0 \cosh k(z + h) \\ Z_n(z, h) &= c_n \cos k_n(z + h) \quad (n \geq 1) \end{aligned} \right\}, \quad (2.3)$$

where k denotes the positive real root of the dispersion relation

$$\nu = k \tanh kh \quad (2.4)$$

and k_n are the positive real roots of

$$\nu = -k_n \tan k_n h, \quad (2.5)$$

arranged such that $k_n < k_{n+1}$ for $n \geq 1$. We also have the coefficients (c_0, c_n) defined by

$$\begin{aligned} c_0 = c_0(h) &= 2\sqrt{k/(2kh + \sinh(2kh))}, \\ c_n = c_n(h) &= 2\sqrt{k_n/(2k_n h + \sin(2k_n h))}, \quad (n \geq 1), \end{aligned}$$

so that the functions $Z_n(z, h)$ ($n \geq 0$) form a complete orthonormal set in the region $-h \leq z \leq 0$. There are also radiation conditions for this scattering problem that follow on from (2.2) and define the solution as $|x| \rightarrow \infty$, which have the form

$$\left. \begin{aligned} \phi(x, z) & (A_- e^{ik_- x} + B_- e^{-ik_- x}) Z_0(z, h_-) \quad x \rightarrow -\infty \\ \phi(x, z) & (A_+ e^{-ik_+ x} + B_+ e^{ik_+ x}) Z_0(z, h_+) \quad x \rightarrow +\infty \end{aligned} \right\}, \quad (2.6)$$

where it is supposed that $h(x) \rightarrow h_{\pm}$ as $x \rightarrow \pm\infty$, and k_{\pm} are the appropriate roots of (2.4) with $h = h_{\pm}$ respectively.

2.1.1 Reflection and Transmission Coefficients

It is with these radiation conditions (2.6) that we can define the reflection and transmission coefficients from the scattering process that we will become more familiar with later. This is done by first choosing the direction of the incident wave.

For a wave incident from the left only we let $A_+ = 0$ and can define the reflection and transmission coefficients, R_- and T_- respectively, by

$$R_- = B_-/A_-, \quad T_- = B_+/A_-.$$

Similarly, by letting $A_- = 0$ describing waves incident from the right only, the corresponding reflection and transmission coefficients are

$$R_+ = B_+/A_+, \quad T_+ = B_-/A_+.$$

Using these two sets of coefficients we can easily define the the amplitudes B_{\pm} of the outgoing waves relative to the incoming wave amplitudes A_{\pm} by

$$\begin{pmatrix} B_- \\ B_+ \end{pmatrix} = S \begin{pmatrix} A_- \\ A_+ \end{pmatrix}, \quad S = \begin{pmatrix} R_- & T_+ \\ T_- & R_+ \end{pmatrix}, \quad (2.7)$$

where S here is the scattering matrix and can provide us with a description of the scattering process. There exist certain relationships between the scattering coefficients that were derived by Newman (1965), namely

$$\left. \begin{aligned} |R_-|^2 + |T_+T_-| &= |R_+|^2 + |T_+T_-| = 1 \\ \arg(T_-) &= \arg(T_+) + 2\alpha_1\pi \\ \arg(R_+R_-) - \arg(T_+T_-) &= \alpha_2\pi \end{aligned} \right\}, \quad (2.8)$$

where α_1 is an integer and α_2 is an odd integer. Another relation that has been proven by Kreisel (1949) is the symmetry relation for reflection where $|R_-| = |R_+|$.

Using these relationships (2.8), we see that by knowing the amplitude A_{\pm} of the incident wave and the amplitude R_{\pm} of the corresponding reflected wave, we can find the amplitude T_{\pm} of the transmitted wave. This is also true if we have T_{\pm} , A_{\pm} and want

to find R_{\pm} , therefore when performing calculations we only need concentrate on either the reflection or transmission coefficients.

2.2 Approximations of the Equations

Here the equations (2.1) are simplified by approximating the vertical structure of the fluid motion so as to remove the z coordinate, called ‘vertically integrated’ models. Approximations of this type have been derived using a variational principle.

Many variational principles have been given, but the form we shall use here is based on Porter and Staziker (1995) and also used by Porter and Chamberlain (1997).

2.2.1 Variational Approximation

Let D be a domain in the plane $z = 0$ with boundary C and define the functional

$$L(\psi) = \frac{1}{2} \int \int_D \left(\nu(\psi^2)_{z=0} - \int_{-h}^0 (\nabla\psi)^2 \right) dx dy.$$

Let $\delta\psi$ denote an arbitrary variation of ψ , then the corresponding first variation of L is given by

$$\begin{aligned} \delta L = & \int \int_D \left\{ -(\delta\psi(\psi_z - \nu\psi))_{z=0} + (\delta\psi(\psi_z + \nabla_h h \cdot \nabla_h \psi))_{z=-h} \right. \\ & \left. + \int_{-h}^0 \delta\psi \nabla^2 \psi dz \right\} dx dy + \int_C \mathbf{n} \cdot \int_{-h}^0 \delta\psi \nabla_h \psi dz dc \end{aligned}$$

where \mathbf{n} is the outward normal unit vector on C . From this it follows that L is stationary for variations $\delta\psi$ which vanish on $C \times [-h, 0]$ if and only if $\psi = \phi$, where ϕ satisfies (2.1) in $D \times [-h, 0]$.

An approximation to find the stationary point of L is done by restricting the choice of ψ to a particular class of functions. Since we are interested here in ‘vertically integrated’

approximations, the general class of functions we require can be written in the form

$$\psi(x, y, z) = \frac{i\omega}{g} \sum_{n=0}^{M-1} \omega_n(h, z) \phi_n(x, y) \quad (2.9)$$

where the functions ω_n are to be assigned. Then the respective functional, given by $L(\psi) = L(\phi_0, \phi_1, \dots, \phi_{M-1})$, is stationary if and only if the functions $\phi_0, \phi_1, \dots, \phi_{M-1}$ satisfy a partial differential equation system which can be arranged into the form

$$\begin{aligned} & \sum_{m=0}^{M-1} \left\{ \nabla_h \cdot \int_{-h}^0 \omega_n \omega_m dz \nabla_h \phi_m \right. \\ & + \left(\int_{-h}^0 \left(\omega_n \frac{\partial \omega_m}{\partial h} - \omega_m \frac{\partial \omega_n}{\partial h} \right) dz \right) \nabla_h h \cdot \nabla_h \phi_m \\ & + \left((\nabla_h h)^2 \left(\frac{d}{dh} \int_{-h}^0 \omega_n \frac{\partial \omega_m}{\partial h} dz - \int_{-h}^0 \frac{\partial \omega_n}{\partial h} \frac{\partial \omega_m}{\partial h} dz \right) \right. \\ & + \int_{-h}^0 \omega_n \frac{\partial^2 \omega_m}{\partial z^2} + \nabla_h^2 h \int_{-h}^0 \omega_n \frac{\partial \omega_m}{\partial h} dz \\ & \left. + (\omega_n \omega_m z)_{z=-h} - (\omega_n (\omega_m z - \nu \omega_m))_{z=0} \right) \phi_m \Big\} \\ & = 0 \quad (n = 0, 1, \dots, M-1). \end{aligned} \quad (2.10)$$

2.2.2 Shallow Water and Mild-Slope Approximations

We shall only be using one-term approximations, whereby the model (2.10) is used with $M = 1$. The first of these, and arguably the simplest, is based on the shallow water hypothesis that wavelength is much greater than the quiescent depth. This is achieved by taking $\omega_0 = 1$, meaning that (2.10) becomes

$$\nabla_h^2 \phi_0 + \nu \phi_0 = 0.$$

This equation supposes that h is continuous, but if we temporarily allow h to be discontinuous then we can obtain a more general result. By returning to the variational

$\delta L = 0$ with $\psi(x, y, z) = \xi(x, y)$ it follows that we have

$$\nabla_h \cdot h \nabla_h \xi + \nu \xi = 0, \quad (2.11)$$

which is the two-dimensional shallow water equation. We shall be using the one-dimensional version of this equation later where instead we have $\xi = \xi(x)$ and $h = h(x)$.

An alternative approximation can be found by instead choosing

$$\omega_0(h, z) = \frac{\cosh k(z + h)}{\cosh(kh)},$$

where the local wavenumber $k = k(h)$ is the corresponding solution of (2.4) with the local depth $h = h(x, y)$. For this choice of ω_0 (2.10) now becomes

$$\nabla_h \cdot u_0 \nabla_h \phi_0 + (u_0 k^2 + u_1 \nabla_h^2 h + u_2 (\nabla_h h)^2) \phi_0 = 0, \quad (2.12)$$

where the coefficients are given by

$$u_0(h) = \int_{-h}^0 \omega_0^2 dz, \quad u_1(h) = \int_{-h}^0 \omega_0 \frac{\partial \omega_0}{\partial h} dz,$$

$$u_2(h) = \frac{d}{dh} u_1(h) - \int_{-h}^0 \left(\frac{\partial \omega_0}{\partial h} \right)^2 dz.$$

Equation (2.12) was derived by Chamberlain (1991) and is known as the modified mild-slope equation. There are many reduced versions of the mild-slope equation that have been derived. The long standing form is given by

$$\nabla_h \cdot u_0 \nabla_h \phi_0 + k^2 u_0 \phi_0 = 0, \quad (2.13)$$

which can be derived from (2.12) by deleting terms $O(\nabla_h^2 h, (\nabla_h h)^2)$ since by the mild-slope approximation we have that $\nabla_h h / kh = O(\epsilon)$, where $\epsilon \ll 1$. Although (2.13) is widely used we shall use the modified mild-slope equation since we would expect the full variational approximation to be superior to a reduced form.

Equation (2.12) is an equation for the two-dimensional wave scattering problem but

since we are only investigating a plane wave parallel to the x -axis, we shall be using the one-dimension version of (2.12) where $h = h(x)$ and $\phi_0 = \phi_0(x)$.

Chapter 3

Forward Wave Scattering

In this chapter we are concerned with finding the reflection coefficient, R , as defined in section 2.1.1. We will assume that we know the amplitude of the incident wave and also that we know the bed topography $h = h(x)$ for $x \in [0, l]$, and that

$$h(x) = \begin{cases} h_a & x < 0, \\ h_b & x > l, \end{cases} \quad (3.1)$$

where h_a and h_b are known constants, i.e. the depth at $x = 0$, $x = l$ can be measured. We also need to choose $\nu = \omega^2/g$ for some range (ν_1, ν_2) say, and then seek to find

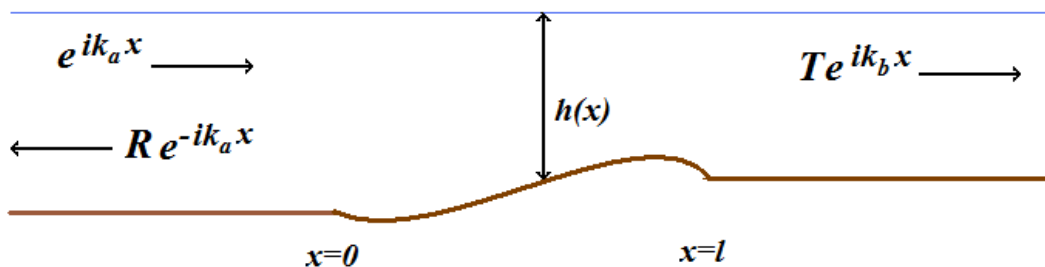


Figure 3.1: Graphical representation of the forward scattering problem, where R and T are the reflection and transmission amplitudes respectively and $h(x)$ is the quiescent depth.

$R = R(\nu)$ for all $\nu \in (\nu_1, \nu_2)$.

The particular problem that we shall be looking at is the case when we have a plane wave incident from the left, which is affected by the bed topography and causes both reflection and transmission waves as shown in Figure 3.1. It is these amplitudes, R and T that we are trying to find, and this is known as *forward scattering*. As shown in section 2.1.1 we need only solve for R or T , not both since they are connected by certain relationships (2.8). So by knowing the incident and reflection amplitudes, the transmission amplitude can be deduced.

3.1 Shallow Water Approximation

For shallow water wave scattering we shall use the one-dimensional case of the approximate equation (2.11) to (2.1), giving

$$(h\phi')' + \nu\phi = 0, \quad (3.2)$$

where the local wave number is given by $k^2(x) = \nu/h(x)$ ¹. We shall just look at the simple case where $h_a = h_b$, therefore $k_a = k_b = \sqrt{\nu/h_a}$.

Using (2.6) as a basis, we can define the solution of $\phi(x)$ as $|x| \rightarrow \infty$ in terms of incident, reflection and transmission waves (as depicted in Figure 3.1). Therefore

$$\phi(x) = \begin{cases} I(e^{ik_ax} + Re^{-ik_ax}) & x < 0, \\ ITe^{ik_a(x-l)} & x > l, \end{cases} \quad (3.3)$$

and since $h(x)$ is constant for $x \in (-\infty, 0) \times (l, \infty)$ we can write the radiation solution (3.3) for $x < 0$ and $x > l$, instead of $x \rightarrow -\infty$ and $x \rightarrow \infty$ respectively.

¹This is derived from the dispersion relation (2.4) where $\tanh kh$ is approximated by kh using the shallow water hypothesis $kh \ll 1$.

3.1.1 Formulating the Problem

Using (3.2) and (3.3) we can formulate the boundary value problem

$$\left. \begin{aligned} \eta'' + k^2\eta &= 0 & (0 < x < l) \\ \eta'(0) + ik_a\eta(0) &= 2ik_a \\ \eta'(l) - ik_a\eta(l) &= 0 \end{aligned} \right\}, \quad (3.4)$$

where we define $\eta = h\phi'$. As shown by Chamberlain (1993), (3.4) can be formulated as the integral equation

$$\begin{aligned} \eta(x) &= e^{ik_ax} - \frac{i}{2k_a} \int_0^l e^{ik_a|x-t|} (k_a^2 - k^2(t))\eta(t)dt, \\ &= e^{ik_ax} - \frac{i\nu}{2k_a} \int_0^l e^{ik_a|x-t|} \rho(t)\eta(t)dt, \quad \rho(t) = \frac{1}{h_a} - \frac{1}{h(t)}. \end{aligned} \quad (3.5)$$

We note here that the lower and upper integration limits of (3.5) can be changed to $-\infty$ and ∞ , since $\rho(t) = 0$ for $t < 0$, $t > l$.

Finally we need to rearrange the equations we have so that we can find R . To do this we consider

$$\eta(0) = h(0)\phi'(0) = ik_a h_a I(1 - R),$$

then, without loss of generality, we choose $I = 1/ik_a h_a$ giving $\eta(0) = 1 - R$. Using this fact and (3.5) implies that

$$R = \frac{i\nu}{2k_a} \int_0^l e^{ik_at} \rho(t)\eta(t)dt = \frac{i\nu}{2k_a} \int_0^\infty e^{ik_at} \rho(t)\eta(t)dt. \quad (3.6)$$

We now have all that we need to solve the forward wave scattering process for shallow water. The procedure that we will follow is;

- Suppose the geometry of the problem is fixed, i.e. l and $h(t)$,
- Allow ν to vary in the chosen interval (ν_1, ν_2) ,
- For each ν , find η by solving either (3.4) or (3.5),

- Using η we can find $R = R(\nu)$ from (3.6).

It is important to note at this point that (3.5) and (3.6) can be conveniently written as

$$\eta(x) = e^{ik_a x} + (M(\rho)\eta)(x), \quad R(\nu) = (N(\eta)\rho)(\nu),$$

where we define the operators $M = M(\rho) : L_2(0, \infty) \rightarrow L_2(0, \infty)$ and $N = N(\eta) : L_2(0, \infty) \rightarrow L_2(0, \infty)$.

3.1.2 Difficulties For Large ν

Here we are concerned with knowing how R changes with ν , where we would expect that $|R| < 1$ and also that $|R| \rightarrow 0$ as $\nu \rightarrow \infty$ which can be seen in Figure 3.2. We expect $|R| < 1$ because this amplitude is relative to the incident wave, and the amplitude of the reflected wave should not be greater than that of the incident.

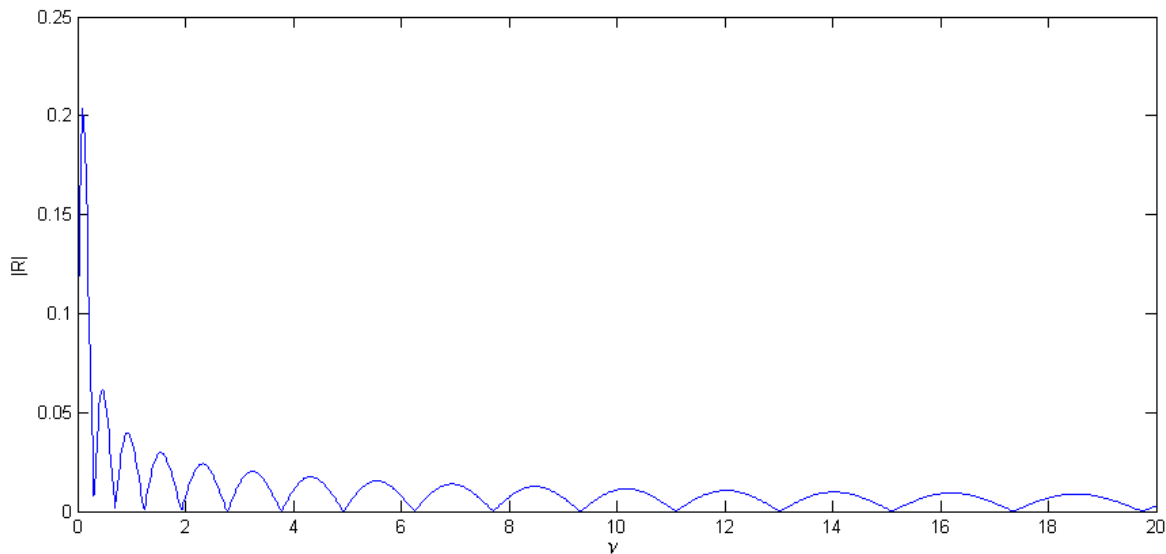


Figure 3.2: Plot of $|R(\nu)|$ using the shallow water approximation, where $l = 5$ and $h(x) = 0.2 - 0.05 \times \sin(2\pi x/5)$

We also expect $|R|$ to be small for large $\nu = \omega^2/g$ (where ω is wave frequency) because waves with large frequencies have small wavelengths, and hence would not be

affected by the bed topography meaning there would be little to no reflection. However in this case, shallow water, it is not applicable to be talking about large ν since in the dispersion relation (2.4) we have assumed that $kh \ll 1$ implying that $\tanh kh \approx kh$. By taking ν to be large implies that k is large and hence this assumption is no longer valid.

Because it is not very accurate to use the shallow water approximation for large ν , we need to use a more accurate approximation so that talking about the behaviour of $|R|$ as $\nu \rightarrow \infty$ makes sense.

3.2 Mild-Slope Approximation

We now attempt to achieve greater accuracy by removing the restriction to shallow water. For this we look at the modified mild slope equation (2.12) for the one-dimensional case $\phi_0 = \phi_0(x)$ and $h = h(x)$, giving

$$(u_0\phi_0')' + (k^2u_0 + h''u_1 + (h')^2u_2)\phi_0 = 0,$$

where $u_{0,1,2}$ are defined as for (2.12) and $k = k(h)$ satisfies the dispersion relation (2.4). Following Porter (2003), we can define $\phi = k\sqrt{u_0}\phi_0$ so that

$$(k^{-2}\phi')' + (1 + (h')^2u_0)\phi = 0,$$

which is approximated by the new mild-slope equation

$$(k^{-2}\phi')' + \phi = 0. \tag{3.7}$$

As with the shallow water approximation, we are again going to take the simple case where $h_a = h_b$ and introduce an incident wave from the left with amplitude I . Hence we may again write

$$\phi(x) = \begin{cases} I(e^{ik_ax} + Re^{-ik_ax}) & x < 0 \\ ITe^{ik_a(x-l)} & x > l \end{cases}, \tag{3.8}$$

where coefficients R and T are related to the reflection and transmission coefficients in (2.7).

3.2.1 Formulating the Problem

In a similar way as for the shallow water case, using (3.7) with (3.8) we can create the boundary problem

$$\left. \begin{aligned} \eta'' + k^2\eta &= 0 & (0 < x < l) \\ \eta'(0) + ik_a\eta(0) &= 2ik_a \\ \eta'(l) - ik_a\eta(l) &= 0 \end{aligned} \right\}, \quad (3.9)$$

where $\eta = k^{-2}\phi'$. Following Chamberlain (1993), we can create an equivalent integral equation to (3.9) given by

$$\eta(x) = e^{ik_ax} - \frac{i}{2k_a} \int_0^l e^{ik_a|x-t|} \rho(t)\eta(t)dt, \quad \rho(t) = k_a^2 - k^2(h(t)). \quad (3.10)$$

To recover R , as with the shallow water case, we can consider

$$\eta(0) = \frac{1}{k^2(h(0))} \phi'(0) = \frac{ik_a}{k_a^2} I(1 - R) = \frac{-1}{ik_a} I(1 - R),$$

and so, without loss of generality, take $I = -ik_a$ so that we have $\eta(0) = 1 - R$. Using this implies that

$$R = \frac{i}{2k_a} \int_0^l e^{ik_at} \rho(t)\eta(t)dt = \frac{i}{2k_a} \int_0^\infty e^{ik_at} \rho(t)\eta(t)dt, \quad (3.11)$$

where we can replace the upper integration limit by ∞ , since $\rho(t) = 0$ for $t > l$.

Now that we have found the governing equations, we can again define the procedure for the forward wave scattering process by;

- Suppose the geometry of the problem is fixed, i.e. l and $h(t)$,
- Allow ν to vary in the chosen interval (ν_1, ν_2) ,
- For each ν , find η by solving either (3.9) or (3.10),
- Using η we can find $R = R(\nu)$ from (3.11).

For convenience later, we can write (3.10) and (3.11) as

$$\eta(x) = e^{ik_a x} + (P(\rho)\eta)(x), \quad R(\nu) = (Q(\eta)\rho)(\nu)$$

respectively, where we define the integral operators $P = P(\rho) : L_2(0, \infty) \rightarrow L_2(0, \infty)$ and $Q = Q(\eta) : L_2(0, \infty) \rightarrow L_2(0, \infty)$.

3.2.2 The Behaviour of R

The forward scattering problem is concerned with the behaviour of R for $\nu \in (\nu_1, \nu_2)$. What we would again expect is that $|R| < 1$ for all $\nu \in (0, \infty)$, since a reflected wave should not have a greater amplitude than the incident wave. We would also expect that $|R| \rightarrow 0$ as $\nu \rightarrow \infty$, since waves of this type would be too small to be affected by the bed topography, and hence not reflect.

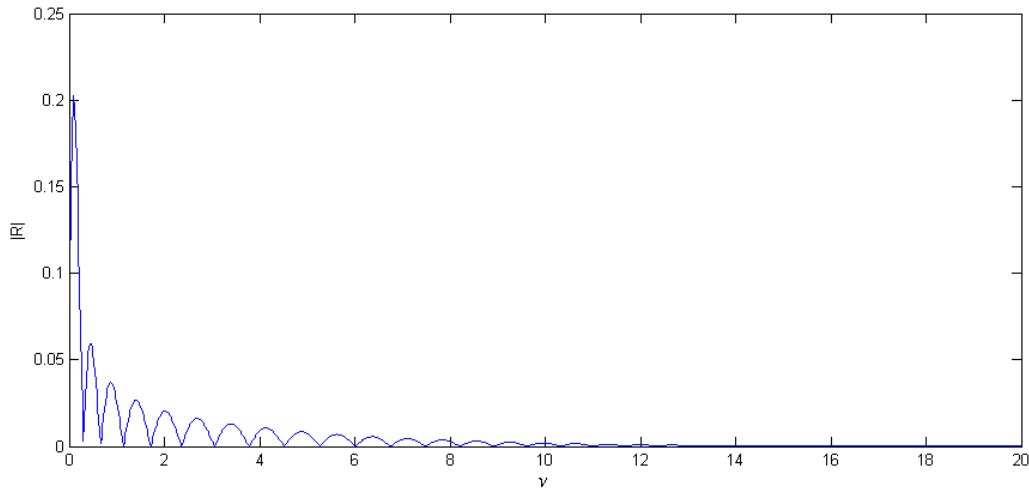


Figure 3.3: Plot of $|R(\nu)|$ using the mild-slope approximation, where $l = 5$ and $h(x) = 0.2 - 0.05 \times \sin(2\pi x/5)$

This expected behavior can be seen in Figure 3.3, but we notice that ν does not have to be that large for $|R|$ to be approximately equal to zero. This in fact appears to happen for $\nu \geq 11$ in this particular example.

We can analyse the behavior of $|R|$ as $\nu \rightarrow \infty$ by looking at (3.11) and taking the absolute value, giving

$$\begin{aligned}
|R| &= \left| \frac{i}{2k_a} \int_0^l e^{ik_a t} \rho(t) \eta(t) dt \right| \leq \frac{1}{2k_a} \left| \int_0^l e^{ik_a t} \rho(t) \eta(t) dt \right|, \\
&\leq \frac{1}{2k_a} \int_0^l |e^{ik_a t} \rho(t) \eta(t)| dt, \\
&\leq \frac{1}{2k_a} \int_0^l |\rho(t)| \cdot |\eta(t)| dt, \\
&\leq \frac{1}{2k_a} \int_0^l |k_a^2 - k^2(h(t))| \cdot |\eta(t)| dt, \\
&\leq \frac{\|\eta\|_\infty}{2k_a} \int_0^l |k_a^2 - k^2(h(t))| dt, \tag{3.12}
\end{aligned}$$

where $\|\eta\|_\infty = \sup_{t \in [0, l]} \{|\eta(t)|\}$.

In this form, (3.12) is difficult to evaluate as $\nu \rightarrow \infty$, therefore we use Taylor's Theorem to attain the approximation

$$k_a^2 - k^2(t) \approx (h_a - h(t)) \left[2k \frac{\partial k}{\partial h} \right]_{h=h_\theta} = \frac{-4k_\theta^3(h_a - h(t))}{2k_\theta h_\theta + \sinh 2k_\theta h_\theta}, \tag{3.13}$$

where $h_\theta = h(\theta)$, $k_\theta = k(h_\theta)$ for some $0 \leq \theta \leq t$. Placing (3.13) back into (3.12) gives

$$\begin{aligned}
|R| &\leq \frac{\|\eta\|_\infty}{2k_a} \int_0^l \left| \frac{4k_\theta^3(h_a - h(t))}{2k_\theta h_\theta + \sinh 2k_\theta h_\theta} \right| dt, \\
&= \frac{2k_\theta^3}{k_a(2k_\theta h_\theta + \sinh 2k_\theta h_\theta)} \|\eta\|_\infty \int_0^l |h_a - h(t)| dt, \\
&\leq \frac{2k_\theta^3 l}{k_a(2k_\theta h_\theta + \sinh 2k_\theta h_\theta)} \|\eta\|_\infty \|h_a - h\|_\infty, \tag{3.14}
\end{aligned}$$

where $\|h_a - h\|_\infty = \sup_{t \in (0, l)} \{|h_a - h(t)|\}$. Using the dispersion relation (2.4) we also find

$$|\nu| = |k_\theta \tanh k_\theta h_\theta| \leq k_\theta |\tanh k_\theta h_\theta| \leq k_\theta, \tag{3.15}$$

therefore $\nu \rightarrow \infty$ implies $k_a \rightarrow \infty$. With this result and (3.14) it is readily seen that $|R| \rightarrow 0$ as $\nu \rightarrow \infty$. Furthermore, by looking at (3.14), we see that the leading term is

$1/\sinh 2k_\theta h_\theta$ as $\nu \rightarrow \infty$. Therefore we see that, for large ν

$$|R| \approx e^{-2k_\theta h_\theta}. \quad (3.16)$$

3.3 Implementation

There are many ways in which this problem could be implemented. For example, (3.4) or (3.9) could be found using a boundary value problem (BVP) solver (for example `bvp4c` MATLAB command). Alternatively (3.5) or (3.10) could be solved, possibly using a numerical scheme for integral equations.

The method that has been used to attain these results is to solve the BVP systems (3.4) and (3.9) by summing together two linearly independent solutions, η_1 and η_2 , that satisfy

$$\eta_j'' + k^2 \eta_j = 0 \quad (j = 1, 2)$$

where

$$\eta_1(0) = 0, \eta_1'(0) = 1 \quad \text{and} \quad \eta_2(0) = 1, \eta_2'(0) = 0.$$

Using these initial conditions we see that the Wronskian is

$$\eta_1(0) \cdot \eta_2'(0) + \eta_1'(0) \cdot \eta_2(0) \neq 0,$$

meaning that these are linearly independent solutions and may be summed together to make a third solution

$$\eta(x) = C_1 \eta_1(x) + C_2 \eta_2(x),$$

where C_1, C_2 are constants that can be found using the boundary conditions defined in (3.4) or (3.9) and can be shown to be

$$C_1 = ik_a(2 - C_2), \quad C_2 = \frac{2(ik_a \eta_1'(l) + k_a^2 \eta_1(l))}{ik_a(\eta_2(l) + \eta_1'(l)) + k_a^2 \eta_1(l) - \eta_2'(l)}.$$

The functions $\eta_{1,2}$, and constants $\eta_{1,2}(l), \eta'_{1,2}(l)$, can be found using an ordinary differential equation solver. The solver that has been used in this case is `ode45` in

MATLAB which gives a numerical solution using Runge Kutta 4 and 5 schemes.

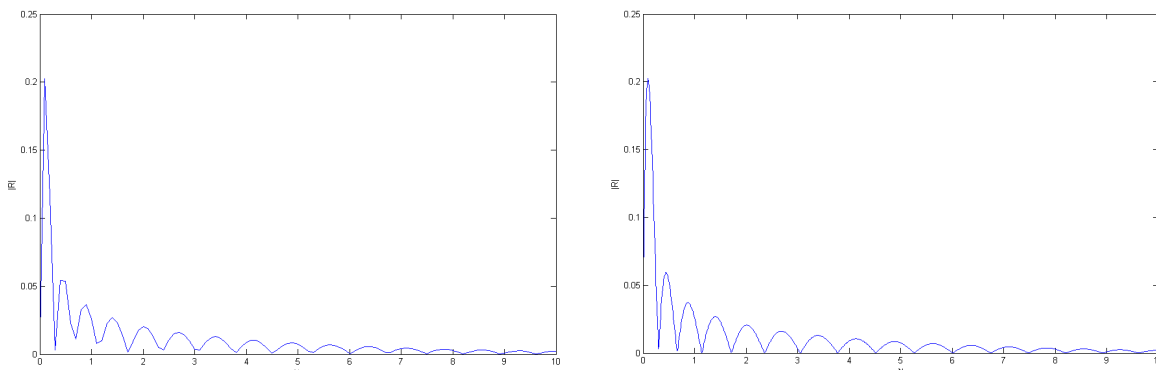


Figure 3.4: Plots of $|R(\nu)|$, where $l = 5$ and $h(x) = 0.2 - 0.05 \times \sin(2\pi x/5)$ with $M = 100$ and $M = 1000$ respectively

The domain $x \in [0, l]$, is divided into N equal sections using $(N + 1)$ nodes and the range of $\nu \in (\nu_1, \nu_2)$ is divided into M equal sections using $(M + 1)$ nodes. In this case we have set $N = 100$ and looked at the results of $|R|$ with different values of M .

In Figure 3.4 we can see that with $M = 100$, some of the information about R has been lost because the discretisation of (ν_1, ν_2) is not fine enough. Comparing this with the $M = 1000$ case we see that there is a lot more data, hence more accuracy, and this will be important later for the inverse wave scattering problem.

3.4 Extensions

The work that we have already shown so far in this chapter assumes that $h_a = h_b$, but this is merely a simple case. So we now allow $h_a \neq h_b$ and will investigate the problem using the mild slope approximation as it has proven to be more accurate than the shallow water approximation. Therefore we shall be using (3.7) with the dispersion relation (2.4) and, for $x < 0$, $x > l$ we have ϕ given by (3.8).

We can define $\eta = k^{-2}\phi$ which solves the boundary value problem

$$\left. \begin{aligned} \eta'' + k^2\eta &= 0 & (0 < x < l) \\ \eta'(0) + ik_a\eta(0) &= 2ik_a \\ \eta'(l) - ik_b\eta(l) &= 0 \end{aligned} \right\}, \quad (3.17)$$

where k_a and k_b are local wavenumbers found using (2.4), evaluated at $h = h_a$ and $h = h_b$ respectively. It can be shown that (3.17) is equivalent to

$$\begin{aligned} \eta(x) = & \left(\frac{k_a}{k_*} + \frac{1}{2} \left(1 - \frac{k_a}{k_*} \right) \eta(0) \right) e^{ik_*x} + \frac{1}{2} \left(1 - \frac{k_b}{k_*} \right) \eta(l) e^{ik_*(l-x)} \\ & - \frac{i}{2k_*} \int_0^l e^{ik_*|x-t|} (k_*^2 - k^2(t)) \eta(t) dt, \end{aligned} \quad (3.18)$$

where we choose the constant $k_* > 0$. By choosing $k_* = k_b$ (3.18) becomes

$$\begin{aligned} \eta(x) &= \left(\frac{k_a}{k_b} + \frac{1}{2} \left(1 - \frac{k_a}{k_b} \right) \eta(0) \right) e^{ik_bx} - \frac{i}{2k_b} \int_0^l e^{ik_b|x-t|} (k_b^2 - k^2(t)) \eta(t) dt \\ &= \left(\frac{k_a}{k_b} + \frac{1}{2} \left(1 - \frac{k_a}{k_b} \right) \eta(0) \right) e^{ik_bx} - \frac{i}{2k_b} \int_0^\infty e^{ik_b|x-t|} (k_b^2 - k^2(t)) \eta(t) dt, \end{aligned} \quad (3.19)$$

where we can replace the upper integration limit by ∞ because $h(x) = h_b$ for $x > l$, therefore $k^2(t) = k_b^2$ for $t > l$.

As with the simpler case, we also have that $\eta(0) = 1 - R$ and therefore

$$R = \frac{k_b - k_a}{k_a + k_b} + \frac{i}{k_a + k_b} \int_0^\infty e^{ik_at} (k_b^2 - k^2(t)) \eta(t) dt. \quad (3.20)$$

This is a more general expression for R , since if we allow $h_a = h_b$ in (3.20) then we get the earlier equation (3.11). Therefore we can think of (3.11) as a special case of (3.20) where $h_a = h_b$.

Chapter 4

Inverse Wave Scattering

In this chapter we are concerned with using given information about the reflection coefficient to approximate the bed topography, $h(x)$ for $x \in (0, l)$.

We shall assume that the reflection coefficient $R = R(\nu)$ for $\nu \in (\nu_1, \nu_2)$ and l are known, and that h_a, h_b can be measured and so also known, as shown in Figure 4.1.

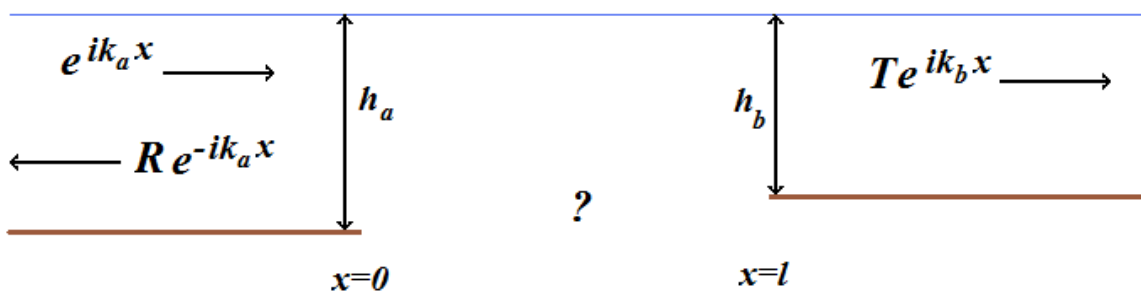


Figure 4.1: Graphical representation of the inverse scattering problem, where R and T are the reflection and transmission amplitudes respectively and $h(x)$, the quiescent depth, is to be found.

The procedure that we shall use to approximate $h(t)$ in this section is an iterative one, whereby if we have an approximation $h_n(t)$ to $h(t)$, we seek to improve this to $h_{n+1}(t)$ by using a number of the equations that we used in Chapter 3 to find $R(\nu)$. We shall be using a scheme of, what we will later come to call, ‘inner’ and ‘outer’ iterations

where the inner iterations are used to converge each $h_n(t)$, and the outer iterations are used to get a first approximation to $h_{n+1}(t)$ from the converged value for $h_n(t)$.

4.1 Shallow Water Approximation

We will assume we have the simple case of $h_a = h_b$, and begin by looking at the shallow water case and suppose that we have an approximation $h_n(t)$ to $h(t)$. Then using the integral equation (3.5), given by $\eta(x) = e^{ik_a x} + (M(\rho)\eta)(x)$, we can define the n^{th} approximation to (3.5) by

$$\eta_n(x) = e^{ik_a x} - \frac{i\nu}{2k_a} \int_0^l e^{ik_a|x-t|} \rho_n(t) \eta_n(t) dt, \quad \rho_n(t) = \frac{1}{h_a} - \frac{1}{h_n(t)}. \quad (4.1)$$

Then once we have solved this approximation for η_n we seek to solve

$$R(\nu) = \frac{i\nu}{2k_a} \int_0^l e^{ik_a t} \rho_{n+1}(t) \eta_n(t) dt, \quad (4.2)$$

for $\rho_{n+1}(t)$, where $R(\nu)$ is known. Then it is a simple case of finding $h_{n+1}(t)$ given by

$$h_{n+1}(t) = \frac{h_a}{1 - h_a \rho_{n+1}(t)},$$

which we will be referred to as the ‘outer iteration’. The ‘inner iterations’ as mentioned earlier are concerned with recovering ρ_{n+1} from (4.2) and will be explained later. Before this we must address the issue of a first approximation, $h_1(t)$, to $h(t)$ so that the method described can be used.

4.1.1 A First Approximation - $h_1(t)$

To get things started, let us take the simplest choice of $h_0(t) = h_a$ and then the first iteration can be carried out explicitly. With this choice for h_0 it follows from (4.1) that

$\eta_0(x) = e^{ik_a x}$. Therefore, using (4.2) gives

$$R(\nu) = \frac{i\nu}{2k_a} \int_0^\infty e^{2ik_a t} \rho_1(t) dt, \quad (4.3)$$

which we wish to solve for $\rho_1(t)$. There are two ways that we can do this, either by inverting a sine, or cosine Fourier transform. If we take the real part of (4.3), we get

$$-\operatorname{Re}(R(\nu)) = \frac{\nu}{2k_a} \int_0^\infty \sin(2k_a t) \rho_1(t) dt,$$

which we can solve for $\rho_1(t)$ by inverting a Fourier sine transform. If we let $\lambda = 2k_a$, then inverting this gives

$$\begin{aligned} \rho_1(t) &= \frac{-4}{\pi} \int_0^\infty \frac{k_a \operatorname{Re}(R(\nu))}{\nu} \sin(\lambda t) d\lambda \\ &= \frac{-4}{h_a \pi} \int_0^\infty \frac{\operatorname{Re}(R(\nu))}{\nu} \sin(2\sqrt{\nu/h_a} t) d\nu, \end{aligned} \quad (4.4)$$

where we have replaced $d\lambda$ by $d\nu$ using

$$\frac{d\nu}{d\lambda} = \frac{d\nu}{dk_a} \cdot \frac{dk_a}{d\lambda} = k_a h_a.$$

Finally, by rearranging (4.4) we can define the first iterate by

$$h_1(t) = h_a \left(1 + \frac{4}{\pi} \int_0^\infty \frac{\operatorname{Re}(R(\nu))}{\nu} \sin(2\sqrt{\nu/h_a} t) d\nu \right)^{-1}. \quad (4.5)$$

Similarly by taking the imaginary part of (4.3) and inverting a Fourier cosine transform to find $\rho_1(t)$, the first iterate is given by

$$h_1(t) = h_a \left(1 - \frac{4}{\pi} \int_0^\infty \frac{\operatorname{Im}R(\nu)}{\nu} \cos(2\sqrt{\nu/h_a} t) d\nu \right)^{-1}. \quad (4.6)$$

We can use either (4.5) or (4.6) to find the first approximation. However, they will not give the same results, as shown in Figure 4.2. Although the difference between these two solutions is very small, the best choice would be to use the inverse Fourier

sine transform (4.5) because it has the property that $\rho_1(0) = 0$, forcing us to have $h_1(0) = h_a$. We do not have this property with the Fourier cosine transform and so we may not necessarily match the first point $h_1(0)$ as accurately as possible.

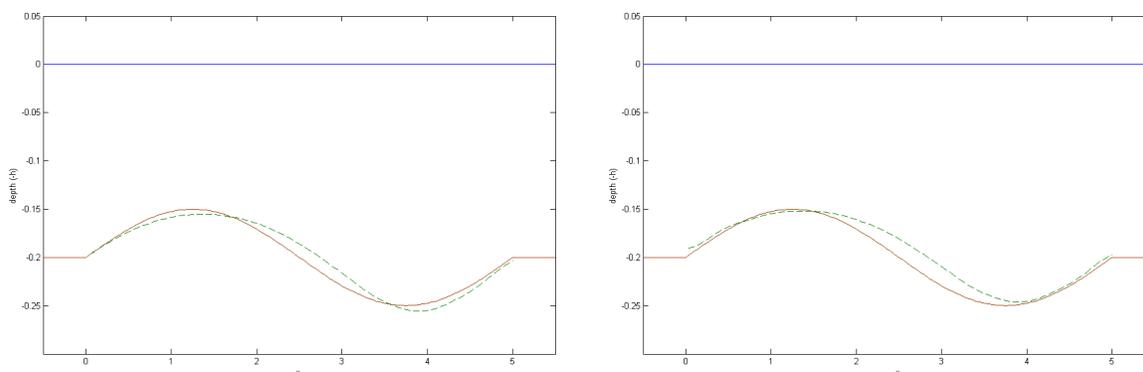


Figure 4.2: $h_1(t)$ (green) as found by (4.5) and (4.6) respectively to approximate bed topography (brown).

Expressions (4.5) and (4.6) are only practical if the integral on the right hand side can be reasonably approximated for $R(\nu)$ where $\nu \in (\nu_1, \nu_2)$. This is related to the problem as noted earlier that the shallow water equations no longer make sense when we begin to talk about $\nu \rightarrow \infty$. The effect of this shall be investigated later.

Now that we have a first iterate $h_1(t)$, we can fully define the method for subsequent iterations.

4.1.2 Further Approximations - $h_{n+1}(t)$

Finding further approximations $h_{n+1}(t)$, to $h(t)$ requires a little more work than for the first approximation, $h_1(t)$, because the integral equation (4.2) is harder to deal with since we may not have that $\rho_n = 0$. The method that we shall use is to approximate each outer iterate, ρ_{n+1} , by an inner iteration.

We begin by noting that (4.1) can be written in the operator form $\eta_n(x) = e^{ik_a x} + (M(\rho_n)\eta_n)(x)$, as described in 3.1.1. Then using $h_n(t)$, we solve (4.1) for η_n and place

this into (4.2) giving

$$\begin{aligned} R(\nu) &= \frac{i\nu}{2k_a} \int_0^l e^{ik_a t} \rho_{n+1}(t) (e^{ik_a t} + (M(\rho_n)\eta_n)(t)) dt \\ &= \frac{i\nu}{2k_a} \int_0^l e^{2ik_a t} \rho_{n+1}(t) dt + \frac{i\nu}{2k_a} \int_0^l e^{ik_a t} \rho_{n+1}(t) (M(\rho_n)\eta_n)(t) dt, \end{aligned}$$

which we use to motivate the ‘inner iteration’

$$\frac{i\nu}{2k_a} \int_0^l e^{2ik_a t} \rho_{n+1}^{(m+1)}(t) dt = R(\nu) - \frac{i\nu}{2k_a} \int_0^l e^{ik_a t} \rho_{n+1}^{(m)}(t) (M(\rho_n)\eta_n)(t) dt \quad (4.7)$$

where we choose $\rho_{n+1}^{(0)} = \rho_n$. To recover $\rho_{n+1}^{(m+1)}$ from (4.7), as for the first approximation case, we can either invert a Fourier sine or cosine transform. For ease let us define

$$F^{(m)}(\nu) = R(\nu) - \frac{i\nu}{2k_a} \int_0^l e^{ik_a t} \rho_{n+1}^{(m)}(t) (M(\rho_n)\eta_n)(t) dt$$

so that using a Fourier sine transform gives

$$\rho_{n+1}^{(m+1)}(t) = -\frac{4}{h_a \pi} \int_0^\infty \frac{\operatorname{Re}(F^{(m)}(\nu))}{\nu} \sin(2\sqrt{\nu/h_a} t) d\nu. \quad (4.8)$$

This is more desirable than using a Fourier cosine transform because we can see from (4.8) that we will always have $\rho_{n+1}(0) = 0$, and so for each approximation n we will have $h_n(0) = h_a$. If we suppose that some stopping criterion is met for the inner iteration when $m = M$ say, for some $M \geq 1$, then we have $\rho_{n+1} = \rho_{n+1}^{(M)}$ and hence can find $h_{n+1} = (h_a^{-1} - \rho_{n+1})^{-1}$.

The procedure that we then use, for the inverse wave scattering problem using a shallow water approximation, is;

- Find the first approximation, $h_1(t)$ to $h(t)$, by using (4.5),
- For $n = 1$ to some stopping criterion $n = N - 1$;
 - Find $\eta_n(x)$ by solving (4.1),
 - Set $\rho_{n+1}^{(0)} = \rho_n$, then for $m = 1$ to some stopping criterion $m = M - 1$;

- * Find $\rho_{n+1}^{(m+1)}$ from (4.8).
- Set $\rho_{n+1} = \rho_{n+1}^{(M)}$,
- Set $h_{n+1} = (h_a^{-1} - \rho_{n+1})^{-1}$.

4.2 Mild-Slope Approximation

By removing the restriction to shallow water and working with the mild-slope approximation we hope to improve the accuracy of the inverse scattering problem. We will assume the simple case where $h_a = h_b$, that we have an approximation $h_n(t)$, to $h(t)$ and are seeking an improved approximation, $h_{n+1}(t)$.

Using h_n we can define an approximation, η_n , to the integral equation (3.10) by

$$\eta_n(x) = e^{ik_a x} - \frac{i}{2k_a} \int_0^l e^{ik_a|x-t|} \rho_n(t) \eta_n(t) dt, \quad (4.9)$$

where $\rho_n(t) = k_a^2 - k_n^2(t)$, and k_n satisfies the dispersion relation (2.4) with $h = h_n(t)$. Once η_n has been approximated we then solve

$$R(\nu) = \frac{i}{2k_a} \int_0^l e^{ik_a t} \rho_{n+1}(t) \eta_n(t) dt \quad (4.10)$$

for $\rho_{n+1}(t)$, and use (2.4) to obtain $h_{n+1} = k_{n+1}^{-1} \tanh^{-1}(\nu k_{n+1}^{-1})$. This procedure will later be referred to as the outer iteration, and the inner iteration deals with extracting ρ_{n+1} from (4.10) and will be described later. Before we can start using this iteration process, we need to create a first approximation, $h_1(t)$, to $h(t)$.

4.2.1 A First Approximation - $h_1(t)$

As for the shallow water case, we can carry out the first outer iteration explicitly with a simple choice of $h_0(t) = h_a$, so that from (4.9) we have $\eta_0(x) = e^{ik_a x}$. It then follows from (4.10) that

$$R(\nu) = \frac{i}{2k_a} \int_0^\infty e^{2ik_a t} \rho_1(t) dt. \quad (4.11)$$

Solving this equation is more complicated than for the shallow water case because $\rho_1(t)$ depends on ν , and hence we cannot use an inverse Fourier transform directly. Instead we can approximate any $\rho_n(t)$ by

$$\rho_n(t) = k_a^2 - k_n^2(t) \approx (h_a - h_n(t)) \left[2k \frac{\partial k}{\partial h} \right]_{h=h_a} = \frac{-4k_a^3(h_a - h_n(t))}{2k_a h_a + \sinh(2k_a h_a)}, \quad (4.12)$$

which we can place into (4.11). Then taking the real part gives

$$\operatorname{Re}(R(\nu)) = \frac{2k_a^2}{2k_a h_a + \sinh(2k_a h_a)} \int_0^l \sin(2k_a t)(h_a - h_1(t)) dt,$$

which we can invert using an inverse Fourier sine transform leading to

$$\begin{aligned} h_1(t) &= h_a - \frac{2}{\pi} \int_0^\infty \frac{2k_a h_a + \sinh(2k_a h_a)}{k_a^2} \operatorname{Re}(R(\nu)) \sin(2k_a t) dk_a \\ &= h_a - \frac{4}{\pi} \int_0^\infty \frac{\cosh^2(k_a h_a)}{k_a^2} \operatorname{Re}(R(\nu)) \sin(2k_a t) d\nu, \end{aligned} \quad (4.13)$$

where the fact that $0 = k^2 \operatorname{sech}^2(kh) + (d\nu/dk)(\partial k/\partial h)$ has been used to change the integration variable. Similarly we may take the imaginary part of (4.11) and perform a Fourier cosine transform to give

$$h_1(t) = h_a + \frac{4}{\pi} \int_0^\infty \frac{\cosh^2(k_a h_a)}{k_a^2} \operatorname{Im}(R(\nu)) \cos(2k_a t) d\nu. \quad (4.14)$$

So we have two different ways of finding $h_1(t)$, but it is preferable to use (4.13) because it has the property that $h_1(0) = h_a$, thereby making sure that the left hand boundary is exact, whereas (4.14) does not have this property, so neither boundary may be exact.

It is reasonable to assume that these integrals ((4.13) and (4.14)) exist since we have shown earlier in Section 3.2.2 that for large ν , $R(\nu) \approx e^{-2k_a h_a}$, and so decays exponentially as $\nu \rightarrow \infty$.

4.2.2 Further Approximations - $h_{n+1}(t)$

Finding further approximations, $h_{n+1}(t)$, to $h(t)$ are more complicated than for the first approximation h_1 since we may no longer have $\rho_n(t) = 0$ and so η_n is not as simple. Firstly it is convenient to note that (4.9) can be written in operator form as $\eta_n(x) = e^{ik_a x} + (P(\rho_n)\eta_n)(x)$.

Using $h_n(t)$ we solve (4.9) for η_n , and placing this into (4.10) gives

$$\begin{aligned} R(\nu) &= \frac{i}{2k_a} \int_0^l e^{ik_a t} \rho_{n+1}(t) (e^{ik_a t} + (P(\rho_n)\eta_n)(t)) dt \\ &= \frac{i}{2k_a} \int_0^l e^{2ik_a t} \rho_{n+1}(t) dt + \frac{i}{2k_a} \int_0^l e^{ik_a t} \rho_{n+1}(t) (P(\rho_n)\eta_n)(t) dt, \end{aligned}$$

which we use to motivate the inner iteration

$$\frac{i}{2k_a} \int_0^l e^{2ik_a t} \rho_{n+1}^{(m+1)}(t) dt = R(\nu) - \frac{i}{2k_a} \int_0^l e^{ik_a t} \rho_{n+1}^{(m)}(t) (P(\rho_n)\eta_n)(t) dt. \quad (4.15)$$

As before, since ρ_{n+1} depends on ν we cannot just use an inverse Fourier transform with the inner iterations in this form. Therefore we use the approximation (4.12) for ρ_{n+1} in (4.15) and rearranging gives the iterative expression

$$\int_0^l e^{2ik_a t} (h_a - h_{n+1}^{(m+1)})(t) dt = \frac{2k_a h_a + \sinh(2k_a h_a)}{2k_a^2} i R(\nu) - \int_0^l e^{ik_a t} (h_a - h_{n+1}^{(m)})(t) (P(\rho_n)\eta_n)(t) dt, \quad (4.16)$$

that we solve for $h_{n+1}^{(m+1)}$. Performing an inverse Fourier sine transform on (4.16) and rearranging gives

$$h_{n+1}^{(m+1)} = h_a - \frac{4}{\pi} \int_0^\infty \frac{\cosh^2(k_a h_a)}{k_a^2} \operatorname{Re}(F^{(m)}(\nu)) \sin(2k_a t) d\nu, \quad (4.17)$$

where

$$F^{(m)}(\nu) = R(\nu) + \frac{2ik_a^2}{2k_a h_a + \sinh(2k_a h_a)} \int_0^l e^{ik_a t} (h_a - h_{n+1}^{(m)})(t) (P(\rho_n)\eta_n)(t) dt.$$

If we suppose that some stopping criterion is met for the inner iteration when $m = M$

say, for some $M \geq 1$, then we have $h_{n+1} = h_{n+1}^{(M)}$.

A Fourier cosine transform could also be used to recover $h_{n+1}^{(m+1)}$, but the sine transform has the property that $h_{n+1}^{(m+1)}(0) = h_a$ for all n and m , whereas the cosine transform does not. This means that the left boundary condition of $h(t)$ will always be imposed in every approximation h_n .

The procedure that we will then use, to solve the inverse water wave scattering problem with a mild-slope approximation, is;

- Find a first approximation $h_1(t)$ using (4.13),
- For $n = 1$ to some stopping criterion $n = N - 1$;
 - Using $h_n(t)$ solve (4.9) for η_n ,
 - Set $h_{n+1}^{(0)} = h_n$, then for $m = 1$ to some stopping criterion $m = M - 1$;
 - * Find $h_{n+1}^{(m+1)}$ from (4.17)
 - Set $h_{n+1} = h_{n+1}^{(M)}$,

4.3 Implementation

To implement this problem, we have first assumed that $R(\nu)$ is known for $\nu \in (\nu_1, \nu_2)$. This is then discretised into M equally spaced parts using $(M + 1)$ nodes, so that in our calculations we use $R(\nu) \approx R(\nu_j)$, where $\nu_j = \nu_1 + j\Delta\nu$ and $\Delta\nu = (\nu_2 - \nu_1)/M$. We also discretise the domain $x \in [0, l]$ into N equally spaced sections using $(N + 1)$ nodes and evaluate at the points $x_j = j\Delta x$, where $\Delta x = l/N$.

The next step is to solve or approximate $\eta_n(x)$ from (4.1), for the shallow water approximation, or (4.9) for a mild-slope approximation. To do this we use a numerical scheme, the *Nyström Method*, which is used to solve integral equations of this type. For the mild-slope approximation this method is given by

$$\eta_n(x_j) = g(x_j) + \sum_{i=0}^N \sigma_i K(x_j, x_i) \eta_n(x_i) \quad j = 0, \dots, N, \quad (4.18)$$

where

$$g(x_j) = e^{ik_a x_j} \quad K(x_j, x_i) = -\frac{i}{2k_a} e^{ik_a |x_j - x_i|} \rho_n(x_i)$$

and σ_i are constants such that $\sigma_0 = \sigma_N = \Delta x/2$, and $\sigma_i = \Delta x$ for $i = 1, \dots, N-1$.

It is clear that (4.18) represents a system an $(N+1)$ equations for the unknowns $\eta_n(x_j)$, $j = 0, \dots, N$.

We introduce the vectors

$$\underline{\eta}_n = \begin{pmatrix} \eta_n(x_0) \\ \vdots \\ \eta_n(x_N) \end{pmatrix}, \quad \underline{g} = \begin{pmatrix} g(x_0) \\ \vdots \\ g(x_N) \end{pmatrix},$$

and the matrix

$$K = \begin{pmatrix} K_{00} & K_{01} & \cdots & K_{0N} \\ \vdots & \vdots & & \vdots \\ K_{N0} & K_{N1} & \cdots & K_{NN} \end{pmatrix},$$

where $K_{ji} = \sigma_i K(x_j, x_i)$. Using these we can rewrite (4.18) and rearrange to find the solution vector, given as

$$\underline{\eta}_n = (I - K)^{-1} \underline{g}.$$

Once $\eta_n(x)$ has been approximated, we use a simple trapezium numerical method to estimate (4.17) in order to find $h_{n+1}^{(m+1)}$. The stopping criterion that we use is to look at the maximum difference between the (m) th and $(m-1)$ th iteration given by

$$\|h_{n+1}^{(m)} - h_{n+1}^{(m-1)}\|_\infty = \max_{j=0, \dots, N} |h_{n+1}^{(m)}(x_j) - h_{n+1}^{(m-1)}(x_j)|,$$

and while this remains larger than a certain threshold, 10^{-16} say, we continue the inner iteration process.

For the shallow water approximation the method is much the same, except that $K(x_j, x_i)$ is defined differently. Also the stopping method for the outer iterations is similar to that for the inner iterations, however we do not yet know if these iterations converge and so these iterations may never meet the stopping criterion. This problem

will be investigated in Chapter 5.

4.4 A Possible Extension

What we have dealt with so far is the simple case where $h_a = h_b$. How can we change the inverse iteration process used for the simple case to solve the far more likely (and complicated) problem when $h_a \neq h_b$? We shall use the mild-slope approximation and suppose that we know $R = R(\nu)$ for $\nu \in (0, \infty)$. We will again be using an iterative process so we shall also suppose that we already have an approximation, $h_n(t)$, and are seeking an improvement, $h_{n+1}(t)$, to $h(t)$.

To begin, we let $k_n = k(h_n)$ be the solution to the dispersion relation (2.4) and then, based on (3.18), we solve the forward problem

$$\eta_n(x) = \gamma_n e^{ik_b x} - \frac{i}{2k_b} \int_0^l e^{ik_b|x-t|} (k_b^2 - k_n^2(t)) \eta_n(t) dt, \quad (4.19)$$

for η_n , where

$$\gamma_n = \frac{k_a}{k_b} + \frac{1}{2} \left(1 - \frac{k_a}{k_b} \right) \eta_n(0).$$

Combining (4.19) with (3.20), we aim to update our approximation to $h(t)$ by using

$$R(\nu) = \frac{k_b - k_a}{k_b + k_a} + \frac{i}{k_b + k_a} \int_0^\infty e^{ik_b t} (k_b^2 - k_{n+1}^2(t)) \eta_n(t) dt, \quad (4.20)$$

so that we can extract $k_{n+1}(t)$. Using this we can obtain $h_{n+1} = k_{n+1}^{-1} \tanh^{-1}(\nu k_{n+1}^{-1})$, and this will be referred to as the outer iteration. The inner iteration is concerned with extracting k_{n+1} from (4.20).

Using (4.19) we can write $\eta_n(t) = \gamma_n e^{ik_b t} + (\eta_n(t) - \gamma_n e^{ik_b t})$, then placing this into

(4.20) we motivate the inner iteration by

$$\begin{aligned}
R(\nu) &= \frac{k_b - k_a}{k_b + k_a} + \frac{i}{k_b + k_a} \int_0^\infty e^{ik_b t} (k_b^2 - k_{n+1}^2(t)) (\gamma_n e^{ik_b t} + (\eta_n(t) - \gamma_n e^{ik_b t})) dt \\
&= \frac{k_b - k_a}{k_b + k_a} + \frac{i\gamma_n}{k_b + k_a} \int_0^\infty e^{2ik_b t} (k_b^2 - k_{n+1}^2(t)) dt \\
&\quad + \frac{i}{k_b + k_a} \int_0^\infty e^{ik_b t} (k_b^2 - k_{n+1}^2(t)) (\eta_n(t) - \gamma_n e^{ik_b t}) dt,
\end{aligned} \tag{4.21}$$

but we cannot invert a Fourier transform as things stand. To make progress we can again use Taylor's theorem to attain the estimate

$$k^2(t) \approx k_b^2 + 2(h - h_b) \left[k \frac{\partial k}{\partial h} \right]_{h=h_b} = k_b^2 - 4(h - h_b) \frac{k_b^3}{2k_b h_b + \sinh(2k_b h_b)}, \tag{4.22}$$

which we can place into (4.21) and rearrange to attain

$$\begin{aligned}
\int_0^\infty e^{2ik_b t} (h_{n+1}^{(m+1)} - h_b) dt &= \frac{2k_b h_b + \sinh(2k_b h_b)}{4ik_b^3 \gamma_n} ((k_b + k_a)R - (k_b - k_a)) \\
&\quad - \gamma_n^{-1} \int_0^\infty e^{ik_b t} (h_{n+1}^{(m)} - h_b) (\eta_n(t) - \gamma_n e^{ik_b t}) dt \\
&= F^{(m)}(k_b).
\end{aligned} \tag{4.23}$$

There are two ways to go from here, we can either invert a Fourier sine or cosine transform and consider real and imaginary parts of (4.23), giving the two possible solutions

$$h_{n+1}^{(m+1)}(t) = h_b + \frac{4}{\pi} \int_0^\infty \operatorname{Re}(F^{(m)}(k_b)) \cos(2k_b t) dt \tag{4.24}$$

$$= h_b + \frac{4}{\pi} \int_0^\infty \operatorname{Im}(F^{(m)}(k_b)) \sin(2k_b t) dt, \tag{4.25}$$

and these steps are referred to as the inner iteration. Suppose that some stopping criterion is met when $m = M$ say, then we complete the inner iteration and perform an outer iteration by setting $h_{n+1} = h_{n+1}^{(M)}$.

We now have the question of how to attain a first approximation $h_1(x)$. One possibility is to follow a similar procedure as for the simple $h_a = h_b$ case, whereby we choose

$h_0(x) = h_b$ so that (4.19) simplifies to give $\eta_0(x) = \gamma_n e^{ik_b x}$. Using this in (4.23) means that we can find h_1 directly without using any inner iterations. This method could pose a problem since it means we are introducing a discontinuity in the solution at $h(0) = h_a$.

An alternative possibility is to choose h_0 as a straight line through the points $h_0(0) = h_a$, $h_0(l) = h_b$. This means that the boundary values have been imposed, so there is no discontinuity, but it also means that there is no cancellation in η_0 so inner iterations will be required to find h_1 .

Chapter 5

Results

In this section we are going to test certain aspects of the inverse scattering iteration process as described in Chapter 4. We shall look at how accurate the shallow water and mild-slope approaches are with respect to estimating each approximation to $h(x)$, $h_n(x)$, and we shall also test the convergence of the inner and outer iterations.

The depth profiles that we shall be using are;

- $h_A(x) = h_a - \epsilon \sin(\frac{2\pi x}{l})$, where we shall choose $h_a = 0.2$, $\epsilon = 0.02$ and $l = 5$.

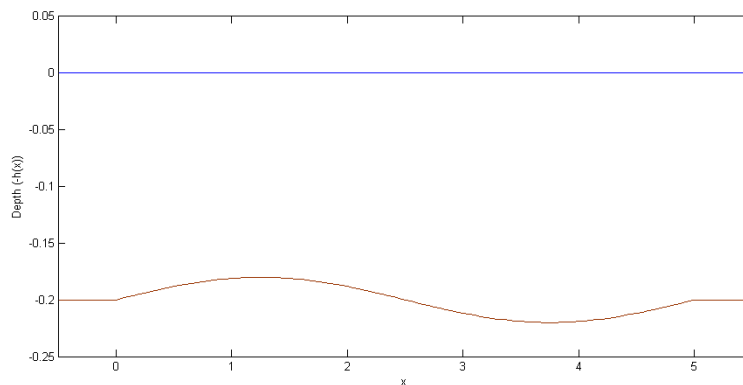
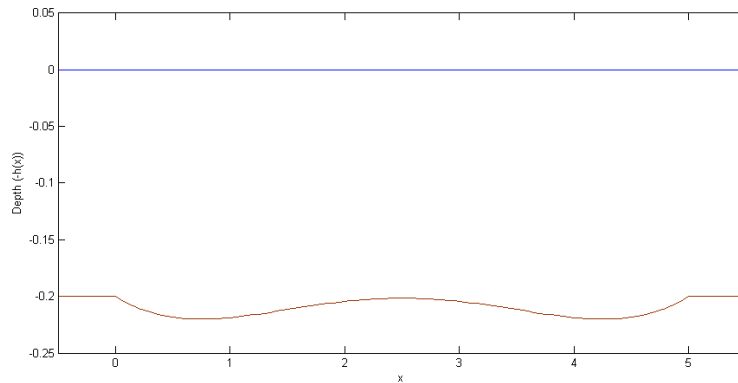
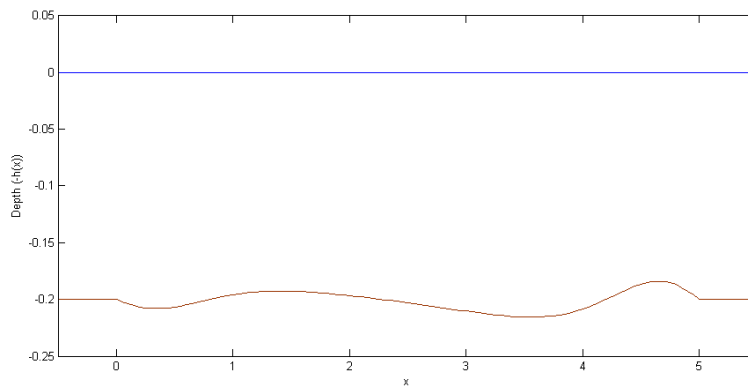


Figure 5.1: Depth profile $h_A(x)$.

- $h_B(x) = h_a \left(1 + 2\epsilon \left(1 - \left(\left(\frac{x}{l} - \alpha \right) \cdot \frac{(x/l)^{-1+\alpha}}{\alpha(1-\alpha)} \right)^2 \right) \right)$, where we shall choose $h_a = 0.2$, $\epsilon = 0.05$, $\alpha = 0.15$ and $l = 5$.

Figure 5.2: Depth profile $h_B(x)$.

- $h_C(x) = h_a (1 + \epsilon \sin(2\pi(x/l)^4) - 0.5\epsilon \sin(2\pi((l-x)/l)^4))$, where we shall choose $h_a = 0.2$, $\epsilon = 0.08$ and $l = 5$.

Figure 5.3: Depth profile $h_C(x)$.

To be able to test the procedure we have formulated to solve the inverse problem we first need to find $R(\nu)$ for $\nu \in (\nu_1, \nu_2)$. We do this by setting the depth profile, $h(x)$ for

$x \in (0, l)$, choose the range (ν_1, ν_2) and then solve the forward scattering problem as in Chapter 3.

5.1 Accuracy of First Approximations $h_1(x)$

To test the accuracy of the first approximations we shall first solve the forward problem to find $R(\nu)$ for $\nu \in (\nu_1, \nu_2)$, where we shall set and fix $\nu_1 = 0.0001$ and allow ν_2 to vary. Using the R that is found we shall use the explicit equations, (4.5) for shallow water and (4.13) for mild slope, to find a first approximation to $h(x)$.

This has been done by firstly discretising the domain $[0, l]$ into N equal sections, with $(N + 1)$ nodes such that at these nodes $x = x_j = j\Delta x$ ($j = 0, \dots, N$), where $\Delta x = l/N$. We then also discretise the domain (ν_1, ν_2) into M equal sections with $(M + 1)$ nodes, then $\Delta\nu = (\nu_2 - \nu_1)/M$. All integrals that are then performed are done so by using numerical schemes, namely a simple trapezium method.

We shall test the accuracy of the first approximation $h_1(x)$ by using the error norms

$$\|h - h_1\|_\infty = \max_{j=0, \dots, N} |h(x_j) - h_1(x_j)|, \quad \|h\|_\infty = \max_{j=0, \dots, N} |h(x_j)|,$$

to find the *relative error* given by $\frac{\|h-h_1\|_\infty}{\|h\|_\infty}$, and we shall also be finding the total error given by

$$\|h - h_1\|_2 = \left(\sum_{j=0}^N |h(x_j) - h_1(x_j)|^2 \right)^{1/2}.$$

5.1.1 Shallow Water Approximation

In this test we have used (4.5) and approximated this integral for $\nu \in (0.0001, \nu_2)$ where we have let $\nu_2 \in [0.1, 20]^1$. We have also set $N = 100$ and $M = 1000$, giving $\Delta x = l/100$ but since we have allowed ν_2 to vary, $\Delta\nu$ is not fixed.

The results obtained from this test are displayed in Table 5.1, and show how the

¹This is reasonable to assume since in (4.5) $R \rightarrow 0$ as $\nu \rightarrow \infty$, and also because the shallow water equations only make sense for small ν .

error between $h(x)$ and $h_1(x)$ varies with the range of ν , and for each bed topography h_A, h_B, h_C . We can see that these errors are not large, but there is still much room for improvement.

ν_2	h_A		h_B		h_C	
	$\frac{\ h-h_1\ _\infty}{\ h\ _\infty}$	$\ h-h_1\ _2$	$\frac{\ h-h_1\ _\infty}{\ h\ _\infty}$	$\ h-h_1\ _2$	$\frac{\ h-h_1\ _\infty}{\ h\ _\infty}$	$\ h-h_1\ _2$
0.1	0.0786	0.0472	0.0677	0.0849	0.0812	0.0762
0.2	0.0386	0.0125	0.0536	0.0368	0.0635	0.0645
0.4	0.0282	0.0114	0.0395	0.0233	0.0404	0.0385
0.6	0.0195	0.0115	0.0377	0.0164	0.0353	0.0371
0.8	0.0191	0.0113	0.0359	0.0162	0.0329	0.0196
1	0.0159	0.0113	0.0364	0.0159	0.0292	0.0204
2	0.0123	0.0108	0.0323	0.016	0.0204	0.0121
4	0.0127	0.0108	0.0295	0.0168	0.0125	0.0076
6	0.0145	0.0112	0.0268	0.018	0.0093	0.0067
8	0.0159	0.0119	0.0241	0.0198	0.0093	0.0065
10	0.0186	0.013	0.0214	0.0225	0.0093	0.0064
12	0.0205	0.0143	0.0209	0.0258	0.0093	0.0064
14	0.0223	0.0156	0.0236	0.0295	0.0093	0.0065
16	0.0245	0.017	0.0259	0.0335	0.0093	0.0067
18	0.0268	0.0184	0.0286	0.0376	0.0097	0.007
20	0.0291	0.0195	0.0309	0.0416	0.0107	0.0073

Table 5.1: Error analysis of $h_1(x)$ as an approximation to $h(x)$ using the shallow water approximation.

We notice that from these results that the smallest values, $\nu_2 = 0.1$, $\nu_2 = 0.2$ give much larger errors, which may be because we have not included enough information from $R(\nu)$ for the approximation to work properly. We can also notice that as ν_2 is increased, the errors begin to decrease to a point and then increase again for $\nu_2 \geq 10$. This could be an effect of the shallow water approximation, meaning that inaccuracies in $R(\nu)$ for larger ν could correspond to the decrease in accuracy as shown in these results (Table 5.1).

5.1.2 Mild-Slope Approximation

As for the shallow water approximation, we are fixing $\nu_1 = 0.0001$ and allowing $\nu_2 \in [0.1, 20]$, then approximating (4.13) between these limits $(\nu_1, \nu_2)^2$. Also, as before, we have set $N = 100$ and $M = 1000$. Therefore we are setting $\Delta x = l/100$ and giving a variable $\Delta\nu$.

The results from finding the error between the first approximation, $h_1(x)$ found using (4.13), and the actual bed topography, $h(x)$, for different ranges of ν are shown in Table 5.2 .

ν_2	h_A		h_B		h_C	
	$\frac{\ h-h_1\ _\infty}{\ h\ _\infty}$	$\ h-h_1\ _2$	$\frac{\ h-h_1\ _\infty}{\ h\ _\infty}$	$\ h-h_1\ _2$	$\frac{\ h-h_1\ _\infty}{\ h\ _\infty}$	$\ h-h_1\ _2$
0.1	0.0464	0.0449	0.0695	0.0881	0.0812	0.0762
0.2	0.0232	0.0187	0.0386	0.0397	0.0631	0.0648
0.4	0.0136	0.0143	0.0286	0.0276	0.0390	0.0379
0.6	0.0109	0.0138	0.0236	0.0187	0.0348	0.0349
0.8	0.0100	0.0137	0.0264	0.0198	0.0315	0.0191
1	0.0095	0.0137	0.0255	0.0186	0.0292	0.0190
2	0.0105	0.0142	0.0282	0.0189	0.0181	0.0098
4	0.0114	0.0159	0.0323	0.0220	0.0102	0.0077
6	0.0123	0.0181	0.0359	0.0262	0.0088	0.0075
8	0.0136	0.0206	0.0395	0.0311	0.0093	0.0078
10	0.0150	0.0233	0.0432	0.0366	0.0088	0.0081
12	0.0164	0.0260	0.0468	0.0424	0.0097	0.0086
14	0.0177	0.0288	0.0509	0.0483	0.0097	0.0091
16	0.0191	0.0314	0.0555	0.0543	0.0102	0.0097
18	0.0205	0.0340	0.0595	0.0603	0.0111	0.0104
20	0.0218	0.0363	0.0632	0.0661	0.0111	0.0111

Table 5.2: Error analysis of $h_1(x)$ as an approximation to $h(x)$ using the mild-slope approximation.

From these results, as for the shallow water case, we can see that for small values of ν_2 the errors are much larger which again may be due to the integral not having enough information from $R(\nu)$ to approximate accurately. We also notice that the approximations, $h_1(x)$, get steadily worse as ν_2 is increased beyond $\nu_2 = 6$. This is not

²This is reasonable since we have shown that $|R(\nu)|$ decays exponentially as $\nu \rightarrow \infty$ (Section 3.2.2).

what we would expect as a result of the mild-slope approximation, and so a possible reason for this problem may be that in our numerical evaluation of (4.13) we are using a variable $\Delta\nu$. If instead we used a fixed $\Delta\nu$ and a variable M we may get better accuracy, which we shall test later.

5.2 Convergence of Iterations

Once a first approximation has been calculated, the inverse scattering process is an iterative one but it is not yet known whether these iterations will converge to the solution $h(x)$. Therefore in this section we are testing the convergence of this iterative process using (4.8) and (4.17), for shallow water and mild slope approximations respectively.

To test for inner iteration convergence we are looking at the maximum error between the $(m)^{\text{th}}$ and $(m-1)^{\text{th}}$ iterates given by

$$\|h_n^{(m)} - h_n^{(m-1)}\|_\infty = \max_{j=0, \dots, N} |h_n^{(m)}(x_j) - h_n^{(m-1)}(x_j)|,$$

and similarly for outer iteration convergence we are looking at the maximum error between the $(n)^{\text{th}}$ and $(n-1)^{\text{th}}$ iterates given by

$$\|h_n - h_{n-1}\|_\infty = \max_{j=0, \dots, N} |h_n(x_j) - h_{n-1}(x_j)|,$$

where we have discretised $h_n(t)$ using $(N+1)$ nodes, and $x_j = j\Delta x$ where $\Delta x = l/N$. For convergence we expect this value to be very small, and decrease to zero as m and n are increased.

We shall also be testing to see if this new approximation, $h_n(x)$, has actually converged to the solution, $h(x)$, that we are looking for, since it may converge to an entirely wrong approximation. To test for this we shall be using the same error norms as used to test the accuracy of the first approximation, $h_1(x)$, and we shall be comparing these to the first approximation in order to ascertain whether this new approximation is more accurate.

5.2.1 Shallow Water Approximation

As for the first approximation, we have found $R(\nu)$ for $\nu \in (\nu_1, \nu_2)$ where we have set $\nu_1 = 0.0001$ and allowed ν_2 to vary. In each case, for numerical computation, we have uniformly discretised ν using $(M + 1)$ nodes meaning that $\Delta\nu = (\nu_2 - \nu_1)/M$ is variable.

Inner Iterations

The results in Table 5.3 show that for $\nu_2 = 0.5$ the inner iteration process is indeed converging to a limit as the number of iterations, m , is increased, for all depth profiles. Table 5.4 also shows that for $\nu_2 = 1$ the inner iteration process is converging. However, the convergence in this case is much slower than for $\nu_2 = 0.5$.

m	$\ h_2^{(m)} - h_2^{(m-1)}\ _\infty$		
	h_A	h_B	h_C
2	2.73×10^{-4}	9.26×10^{-4}	1.18×10^{-4}
3	1.13×10^{-5}	6.49×10^{-5}	6.91×10^{-7}
4	8.51×10^{-7}	4.99×10^{-6}	1.09×10^{-8}
5	3.19×10^{-8}	3.69×10^{-7}	9.27×10^{-11}
10	1.75×10^{-14}	8.18×10^{-13}	0
15	0	2.78×10^{-17}	0

Table 5.3: Error between $(m)^{\text{th}}$ and $(m-1)^{\text{th}}$ iterate with $\nu_2 = 0.5$, using shallow water approximation.

m	$\ h_2^{(m)} - h_2^{(m-1)}\ _\infty$		
	h_A	h_B	h_C
2	7.46×10^{-4}	0.006	0.0014
3	1.07×10^{-4}	0.0015	9.33×10^{-5}
4	1.72×10^{-5}	3.85×10^{-4}	3.76×10^{-6}
5	3.84×10^{-6}	1.03×10^{-4}	2.23×10^{-7}
10	1.04×10^{-9}	1.55×10^{-7}	6.82×10^{-14}
15	2.93×10^{-13}	2.29×10^{-10}	0

Table 5.4: Error between $(m)^{\text{th}}$ and $(m-1)^{\text{th}}$ iterate with $\nu_2 = 1$, using shallow water approximation.

Although the results in Tables 5.3 and 5.4 imply convergence of the inner iteration, we still need to test that they are converging to $h(x)$. If they are indeed converging to

ν_2	\mathbf{h}_A		\mathbf{h}_B		\mathbf{h}_C	
	$\frac{\ h-h_1\ _\infty}{\ h\ _\infty}$	$\frac{\ h-h_2\ _\infty}{\ h\ _\infty}$	$\frac{\ h-h_1\ _\infty}{\ h\ _\infty}$	$\frac{\ h-h_2\ _\infty}{\ h\ _\infty}$	$\frac{\ h-h_1\ _\infty}{\ h\ _\infty}$	$\frac{\ h-h_2\ _\infty}{\ h\ _\infty}$
0.5	0.0232	0.0295	0.0423	0.0605	0.0366	0.0533
1	0.0159	0.0550	0.0364	0.1114	0.0292	0.1257
5	0.0132	1	0.0282	1	0.0102	1.0264

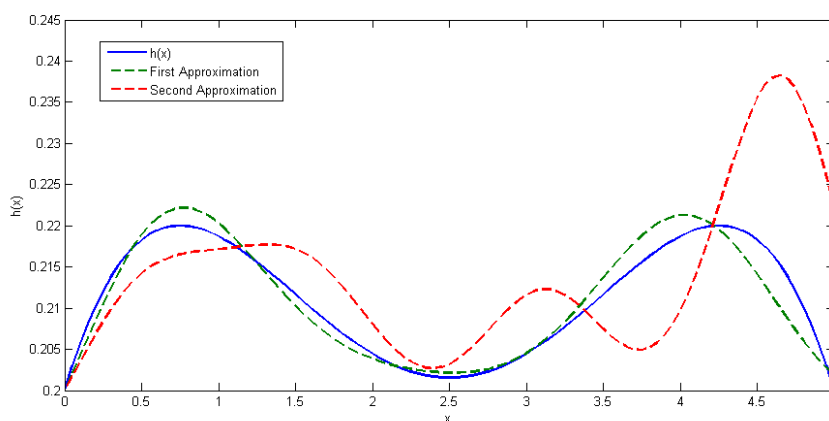
Table 5.5: Comparing the relative error of $h_1(x)$ with $h_2(x)$.

ν_2	\mathbf{h}_A		\mathbf{h}_B		\mathbf{h}_C	
	$\ h-h_1\ _2$	$\ h-h_2\ _2$	$\ h-h_1\ _2$	$\ h-h_2\ _2$	$\ h-h_1\ _2$	$\ h-h_2\ _2$
0.5	0.0124	0.0327	0.0199	0.044	0.0371	0.0535
1	0.0113	0.048	0.0159	0.0908	0.0204	0.1186
5	0.011	2.005	0.0173	2.1137	0.007	0.4691

Table 5.6: Comparing the total error of $h_1(x)$ with $h_2(x)$.

the correct solution we would expect this new approximation to be more accurate than the previous.

In Tables 5.5 and 5.6 we have compared the accuracy of $h_2(x)$ with $h_1(x)$ in approximating $h(x)$. We can see from the results shown that the new approximation is less accurate than the first approximation, in fact we can see that as ν_2 is increased the errors have become very large. From this we can infer that the iteration process fails

Figure 5.4: Comparison of h_1 with h_2 using $h = h_B$ and $\nu_2 = 1$.

for the shallow water approximation if we include larger values of ν , which we would expect since the theory behind this approximation is based on the idea that ν is small compared to the depth.

It is clear to see in Figure 5.4 that the first approximation, $h_1(x)$, is much more accurate than the second approximation, $h_2(x)$, since the second approximation is almost non-recognisable as being an approximation to $h(x)$. The first approximation gives a far more clear and accurate idea as to the shape of $h(x)$.

Outer Iterations

Taking into consideration the fact that the shallow water approximation is far less accurate for large values of ν_2 , we have restricted our investigation of convergence to smaller values. The results shown in Table 5.7 imply that our approximation to $h(x)$ is converging to a solution in all cases, and it also shows that this convergence is faster for smaller ν_2 .

ν_2	n	$\ h_n - h_{n-1}\ _\infty$		
		h_A	h_B	h_C
0.3	3	2.95×10^{-6}	1.09×10^{-5}	3.85×10^{-6}
	4	6.77×10^{-8}	4.39×10^{-7}	1.48×10^{-8}
	5	6.77×10^{-10}	9.82×10^{-9}	4.04×10^{-11}
	6	1.62×10^{-11}	3.54×10^{-10}	1.38×10^{-13}
	7	2.28×10^{-13}	9.08×10^{-12}	5.55×10^{-16}
0.5	3	4.91×10^{-4}	0.0026	0.0012
	4	2.64×10^{-5}	1.82×10^{-4}	6.28×10^{-6}
	5	1.04×10^{-6}	1.37×10^{-5}	5.53×10^{-8}
	6	6.45×10^{-8}	1.00×10^{-6}	3.26×10^{-10}
	7	2.45×10^{-9}	7.15×10^{-8}	1.61×10^{-12}
0.7	3	0.0168	0.0949	0.0319
	4	9.65×10^{-4}	0.0146	5.76×10^{-4}
	5	1.20×10^{-4}	0.0046	1.07×10^{-5}
	6	6.85×10^{-6}	4.44×10^{-4}	2.39×10^{-7}
	7	8.49×10^{-7}	1.38×10^{-4}	5.21×10^{-9}

Table 5.7: Error between $(n)^{\text{th}}$ and $(n-1)^{\text{th}}$ iterate using the shallow water approximation.

Even though the iterations appear to be convergent, we cannot guarantee that what they are converging to is the required solution. To test this we have performed similar error analysis as with the first approximation, the results of which can be seen in Table 5.8. The results show that the approximations, $h_n(x)$, are more accurate for smaller values of ν_2 and that the errors become much larger as ν_2 is increased, which is most likely as a result of the restriction to shallow water.

ν_2	n	\mathbf{h}_A		\mathbf{h}_B		\mathbf{h}_C	
		$\frac{\ h-h_n\ _\infty}{\ h\ _\infty}$	$\ h-h_n\ _2$	$\frac{\ h-h_n\ _\infty}{\ h\ _\infty}$	$\ h-h_n\ _2$	$\frac{\ h-h_n\ _\infty}{\ h\ _\infty}$	$\ h-h_n\ _2$
0.3	2	0.0295	0.0257	0.0509	0.0339	0.0533	0.0421
	3	0.0314	0.0248	0.0523	0.0391	0.0557	0.0439
	4	0.0305	0.0239	0.0500	0.0365	0.0552	0.0435
	5	0.0305	0.024	0.0500	0.036	0.0552	0.0434
	6	0.0305	0.0241	0.0505	0.0363	0.0552	0.0434
	7	0.0305	0.024	0.0505	0.0363	0.0552	0.0435
0.5	2	0.0295	0.0327	0.0605	0.044	0.0533	0.0535
	3	0.0418	0.0347	0.0895	0.0691	0.0566	0.0563
	4	0.0373	0.0271	0.0755	0.054	0.0547	0.0448
	5	0.0336	0.0263	0.0605	0.0311	0.0455	0.0423
	6	0.0359	0.0289	0.0682	0.0402	0.0478	0.0475
	7	0.0368	0.0285	0.0759	0.0501	0.0510	0.0471
0.7	2	0.0364	0.04	0.0805	0.0657	0.0737	0.0561
	3	0.0650	0.0548	0.1641	0.1468	0.0914	0.0951
	4	0.0591	0.0513	0.1232	0.1655	0.0928	0.0846
	5	0.0368	0.0375	0.1245	0.1309	0.0631	0.0833
	6	0.0541	0.0603	0.1736	0.2124	0.1206	0.1232
	7	0.0886	0.0804	0.4027	0.408	0.1609	0.1817

Table 5.8: Error analysis of $h_n(x)$ to $h(x)$ using the shallow water approximation.

By comparing Tables 5.8 and 5.1 we see that the first approximation $h_1(x)$ is more accurate than the other approximations, $h_n(x)$. So for greater accuracy with the shallow water approximation it could be argued that we should simply use the first approximation and not bother with the iterative process, but the errors in this case are still too large.

The inaccuracy of the converged solutions can plainly be seen in Figure 5.5 where,

even though ν_2 gives the smallest errors, the converged solution is a poor approximation to $h(x)$. This is possibly most clear for the case when $h = h_C$.

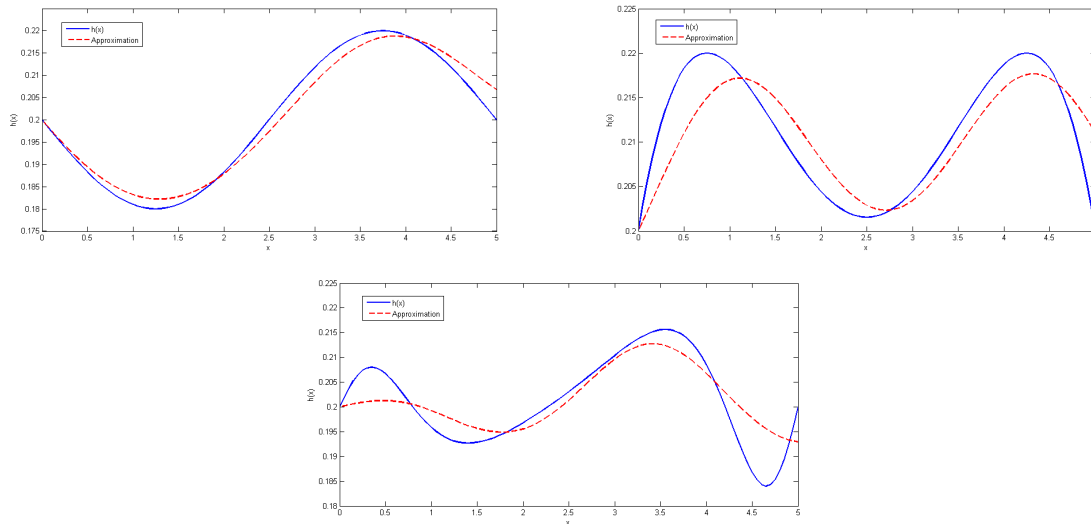


Figure 5.5: Converged depth profiles for h_A , h_B and h_C respectively with $\nu_2 = 0.3$, using the shallow water approximation.

5.2.2 Mild-Slope Approximation

As for the shallow water approximation, we have found $R(\nu)$ for $\nu \in (\nu_1, \nu_2)$ where we have set $\nu_1 = 0.0001$ and allowed ν_2 to vary. In each case, for numerical computation, we have uniformly discretised ν using $(M + 1)$ nodes meaning that $\Delta\nu = (\nu_2 - \nu_1)/M$ is variable, as earlier.

Inner Iterations

From Tables 5.9 and 5.10 we can see that the inner iterations appear to be converging as the number of iterations, m , is increased. Also by comparing Tables 5.9 and 5.10 with 5.3 and 5.4 respectively, we note that the convergence appears to be faster for the mild-slope approximation, and slower for the shallow water approximation. The rate of

	$\ h_2^{(m)} - h_2^{(m-1)}\ _\infty$		
m	h_A	h_B	h_C
2	1.68×10^{-4}	1.30×10^{-4}	2.93×10^{-6}
3	1.40×10^{-5}	8.38×10^{-6}	2.47×10^{-8}
4	8.04×10^{-7}	5.59×10^{-7}	2.73×10^{-10}
5	6.79×10^{-8}	3.96×10^{-8}	2.55×10^{-12}
10	7.82×10^{-14}	5.07×10^{-14}	0
15	2.78×10^{-17}	0	0

Table 5.9: Error between $(m)^{\text{th}}$ and $(m-1)^{\text{th}}$ iterate with $\nu_2 = 0.5$, using mild-slope approximation.

	$\ h_2^{(m)} - h_2^{(m-1)}\ _\infty$		
m	h_A	h_B	h_C
2	2.38×10^{-4}	2.77×10^{-4}	1.96×10^{-5}
3	2.83×10^{-5}	2.53×10^{-5}	4.67×10^{-7}
4	3.10×10^{-6}	2.99×10^{-6}	1.14×10^{-8}
5	4.01×10^{-7}	3.09×10^{-7}	2.78×10^{-10}
10	9.04×10^{-12}	5.63×10^{-12}	2.78×10^{-17}
15	1.94×10^{-16}	1.39×10^{-16}	0

Table 5.10: Error between $(m)^{\text{th}}$ and $(m-1)^{\text{th}}$ iterate with $\nu_2 = 1$, using mild-slope approximation.

	$\ h_2^{(m)} - h_2^{(m-1)}\ _\infty$		
m	h_A	h_B	h_C
2	2.55×10^{-4}	8.31×10^{-4}	1.13×10^{-4}
3	3.14×10^{-5}	2.08×10^{-4}	8.57×10^{-6}
4	5.77×10^{-6}	6.11×10^{-5}	9.15×10^{-7}
5	9.89×10^{-7}	1.56×10^{-5}	7.89×10^{-8}
10	9.70×10^{-10}	3.25×10^{-8}	8.73×10^{-13}
15	3.14×10^{-12}	6.50×10^{-11}	2.78×10^{-17}

Table 5.11: Error between $(m)^{\text{th}}$ and $(m-1)^{\text{th}}$ iterate with $\nu_2 = 10$, using mild-slope approximation.

convergence remains quite fast even when ν_2 is increased, which can be seen in Table 5.11. This, however, was not the case in the shallow water case as a number of iterates diverged creating very spurious results. Although these inner iterations appear to be converging, we still need to check that they are converging to the solution, $h(x)$, and not to some other result (as in the shallow water approximation case).

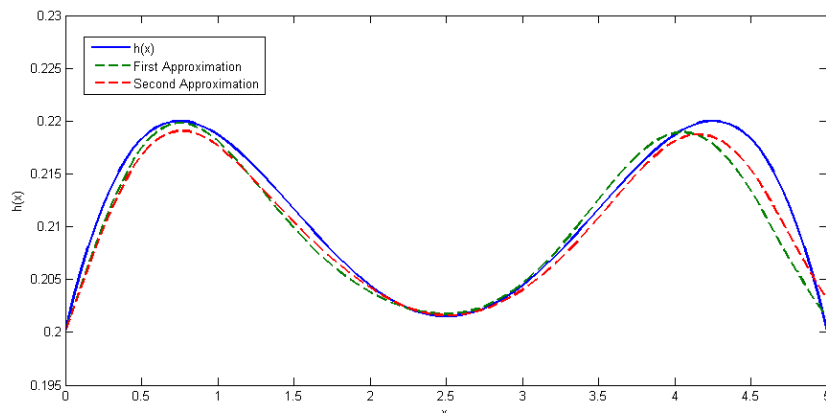
ν_2	\mathbf{h}_A		\mathbf{h}_B		\mathbf{h}_C	
	$\frac{\ h-h_1\ _\infty}{\ h\ _\infty}$	$\frac{\ h-h_2\ _\infty}{\ h\ _\infty}$	$\frac{\ h-h_1\ _\infty}{\ h\ _\infty}$	$\frac{\ h-h_2\ _\infty}{\ h\ _\infty}$	$\frac{\ h-h_1\ _\infty}{\ h\ _\infty}$	$\frac{\ h-h_2\ _\infty}{\ h\ _\infty}$
0.5	0.0127	0.0118	0.0259	0.0241	0.0343	0.0348
1	0.0095	0.0114	0.0255	0.0150	0.0292	0.0311
5	0.0118	0.0127	0.0345	0.0209	0.0083	0.0097
10	0.0150	0.0150	0.0432	0.0373	0.0088	0.0083
15	0.0186	0.0191	0.0532	0.0523	0.0102	0.0102

Table 5.12: Comparing the relative error of $h_1(x)$ with $h_2(x)$.

ν_2	\mathbf{h}_A		\mathbf{h}_B		\mathbf{h}_C	
	$\ h-h_1\ _2$	$\ h-h_2\ _2$	$\ h-h_1\ _2$	$\ h-h_2\ _2$	$\ h-h_1\ _2$	$\ h-h_2\ _2$
0.5	0.0142	0.014	0.0243	0.021	0.0363	0.0362
1	0.0137	0.0136	0.0186	0.0134	0.019	0.0182
5	0.0169	0.0168	0.024	0.019	0.0076	0.0069
10	0.0233	0.0232	0.0366	0.0333	0.0081	0.0075
15	0.0301	0.0301	0.0513	0.0491	0.0094	0.0089

Table 5.13: Comparing the total error of $h_1(x)$ with $h_2(x)$.

Tables 5.12 and 5.13 show the errors between the newly converged $h_2(x)$ and $h(x)$, compared with the error that arose using the first approximation. These results hint at the idea that the new approximation is more accurate than the first, and so the converged limit is in fact tending to the solution $h(x)$.

Figure 5.6: Comparison of h_1 with h_2 using $h = h_B$ and $\nu_2 = 1$.

This certainly appears to be the case when using $h = h_B$ since both the relative and total errors have decreased, and comparing Figure 5.6 with Figure 5.4 it is clear to see that the mild-slope approximation is working much more accurately than the shallow water approximation. However, it is less clear that the inner iterations are converging to $h(x)$ for $h = h_A$ and $h = h_C$, since although some of the total errors may have decreased there are some instances where the maximum error has increased. This is not the desired result, as we would hope to see the maximum error between $h_n(x)$ and $h(x)$ to tend to zero as n is increased.

Outer Iterations

As we did for the shallow water approximation, we now look at the outer iteration process for the mild-slope approximation and attempt to find signs that these iterates are converging and if so, to what solution. From Table 5.14 we can see that the maximum error between the (n^{th}) and ($(n - 1)^{\text{th}}$) outer iteration is small and decreasing to zero as n is increased, which is a good indication that the iterations are converging. Comparing

ν_2	n	$\ h_n - h_{n-1}\ _\infty$		
		h_A	h_B	h_C
1	3	4.97×10^{-8}	3.24×10^{-8}	6.26×10^{-12}
	4	6.23×10^{-9}	3.35×10^{-9}	1.57×10^{-13}
	5	7.38×10^{-10}	3.90×10^{-10}	3.80×10^{-15}
	6	8.85×10^{-11}	4.12×10^{-11}	8.33×10^{-17}
	7	1.09×10^{-11}	4.73×10^{-12}	0
5	3	2.09×10^{-7}	3.24×10^{-6}	6.16×10^{-9}
	4	4.42×10^{-8}	8.92×10^{-7}	5.31×10^{-10}
	5	1.19×10^{-8}	2.34×10^{-7}	4.57×10^{-11}
	6	2.96×10^{-9}	6.61×10^{-8}	3.78×10^{-12}
	7	8.81×10^{-10}	1.75×10^{-8}	3.31×10^{-13}
15	3	2.63×10^{-7}	2.40×10^{-6}	7.81×10^{-9}
	4	6.21×10^{-8}	5.06×10^{-7}	7.20×10^{-10}
	5	1.62×10^{-8}	1.52×10^{-7}	7.18×10^{-11}
	6	4.21×10^{-9}	3.41×10^{-8}	6.48×10^{-12}
	7	1.32×10^{-9}	9.83×10^{-9}	7.03×10^{-13}

Table 5.14: Error between (n^{th}) and ($(n - 1)^{\text{th}}$) iterate using mild-slope approximation.

Tables 5.14 and 5.7 we see that the convergence in the mild-slope approximation case, in general, is much faster and more convincing than in shallow water case. However, we still have the same question as to whether these iterations are in fact converging to the required solution $h(x)$.

In Table 5.15 we can see that the errors between the approximation, $h_n(x)$, and $h(x)$ do not grow or oscillate as in the shallow water approximation case. We also note that most of these errors are smaller than for the corresponding first approximation as shown in Table 5.2, and others are not greatly larger. This was not the case for the shallow water approximation, and so we can see that for the mild-slope approximation the iteration process appears to be improving toward the desired solution.

ν_2	n	\mathbf{h}_A		\mathbf{h}_B		\mathbf{h}_C	
		$\frac{\ h-h_n\ _\infty}{\ h\ _\infty}$	$\ h-h_n\ _2$	$\frac{\ h-h_n\ _\infty}{\ h\ _\infty}$	$\ h-h_n\ _2$	$\frac{\ h-h_n\ _\infty}{\ h\ _\infty}$	$\ h-h_n\ _2$
1	2	0.0114	0.0136	0.0150	0.0134	0.0311	0.0182
	3	0.0114	0.0137	0.0150	0.0137	0.0311	0.0182
	4	0.0114	0.0137	0.0155	0.0138	0.0311	0.0182
	5	0.0114	0.0137	0.0155	0.0138	0.0311	0.0182
5	2	0.0127	0.0168	0.0209	0.019	0.0097	0.0069
	3	0.0132	0.0169	0.0182	0.019	0.0102	0.0068
	4	0.0132	0.0169	0.0182	0.019	0.0102	0.0068
	5	0.0132	0.0169	0.0182	0.019	0.0102	0.0068
15	2	0.0191	0.0301	0.0523	0.0491	0.0102	0.0089
	3	0.0191	0.0302	0.0505	0.049	0.0102	0.0089
	4	0.0191	0.0302	0.0500	0.049	0.0102	0.0089
	5	0.0191	0.0302	0.0500	0.049	0.0102	0.0089

Table 5.15: Error analysis of $h_n(x)$ to $h(x)$ using the mild-slope approximation.

The greater accuracy in the mild-slope approximation over that of the shallow water approximation can also be seen by comparing Figure 5.7 with Figure 5.5 (and also in further results in Appendix A). Here we see that, particularly for $h = h_C$, the mild-slope approximation finds the shape of $h(x)$ far more accurately than in the shallow water approximation.

An interesting point to note here is that in Figure 5.7 (and also in Figures A.7 and A.8 in Appendix A) we can see that the approximations, $h_n(x)$, seem less accurate

at points where $h(x)$ has a local maximum or minimum. It is also possible that the amplitudes of these curves play a part in the accuracy of the approximation, since the turning points in $h = h_C$, that have smaller amplitude, are better approximated than those in $h = h_A$ or $h = h_B$.

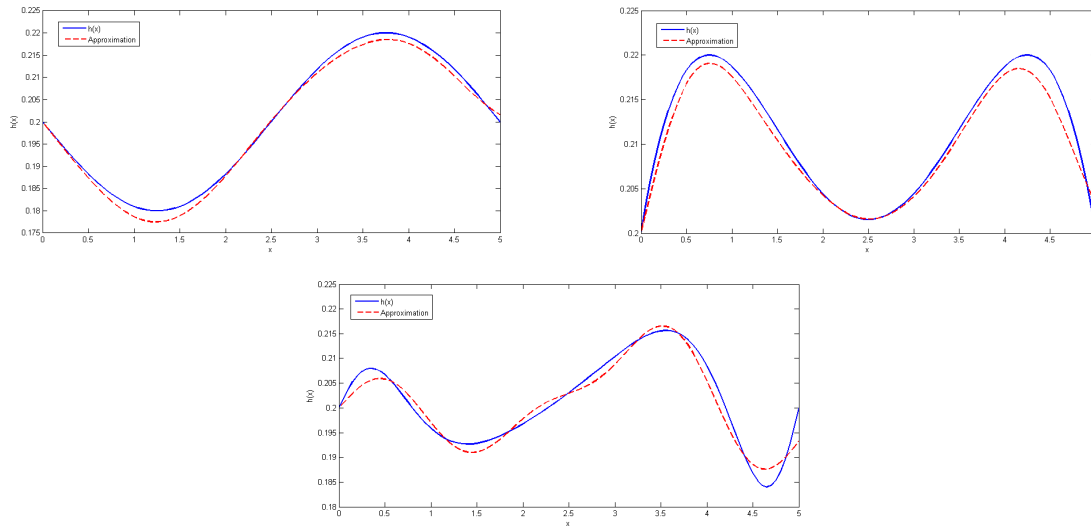


Figure 5.7: Converged depth profiles for h_A , h_B and h_C respectively with $\nu_2 = 1$, using the mild-slope approximation.

5.3 Further Testing

So far we have concerned ourselves with testing the convergence of the iterative processes for the inverse scattering problem and found that of the two approximations used, the mild-slope approximation gave better results. Therefore in this section we are going to restrict our attention to the mild-slope approximation and attempt to understand how the solution obtained behaves when the numerical accuracy of the process is increased, and also what range of (ν_1, ν_2) is required to obtain a reasonable approximation to $h(x)$.

5.3.1 Greater Accuracy?

So far, for numerical computation, we have been discretising the domain (ν_1, ν_2) into M sections using $(M + 1)$ nodes, and let $\nu \approx \nu_j = j\Delta\nu + \nu_1$ for $j = 0, \dots, M$, where $\Delta\nu = (\nu_2 - \nu_1)/M$. This means that in each test we have been using a variable $\Delta\nu$, and for large ranges of (ν_1, ν_2) this would make the discretisation very coarse, possibly leading to errors in the solution. Here we aim to investigate what impact this has by instead fixing $\Delta\nu = 0.001$ and allowing M to vary.

ν_2	$\frac{\ h-h_n\ _\infty}{\ h\ _\infty}$		
	h_A	h_B	h_C
1	0.0114	0.0155	0.0311
5	0.0118	0.0105	0.0097
10	0.0118	0.0091	0.0070
15	0.0118	0.0091	0.0070

Table 5.16: Relative error of converged approximation, $h_n(x)$ to $h(x)$, using the mild-slope approximation and a fixed $\Delta\nu$.

Comparing the results found in Table 5.16 with those in Table 5.15, reveals that by fixing $\Delta\nu$ in this way does in fact improve the accuracy of the approximate solution as ν_2 is increased.

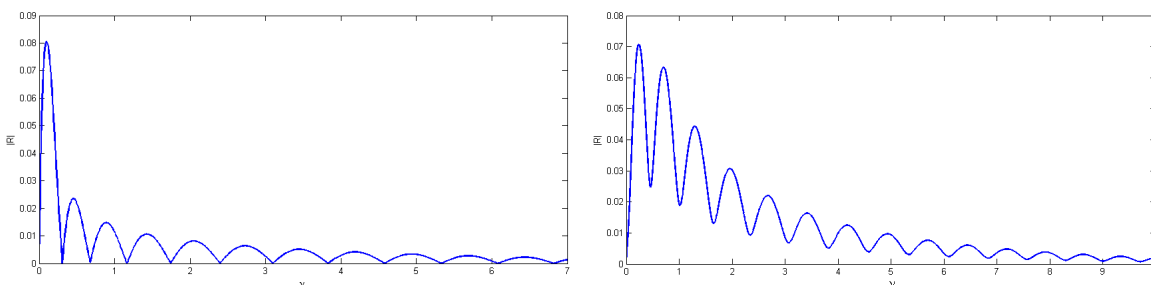


Figure 5.8: $|R(\nu)|$ for $h = h_A$ and $h = h_C$ respectively.

Also from Table 5.16 we can see that after a certain point, for each depth profile, including a larger range for ν does not necessarily improve the accuracy of the found solution. This means that, in a computational sense, we should be able to neglect the

range of ν that appears not effect the accuracy. A possible way to do this is to compare these ‘neglectable’ ranges with the reflected data $R(\nu)$ as shown in Figure 5.8. From here we can see that these ranges correspond to very small values of $|R|$, and in practice we could perhaps only use the range (ν_1, ν_2) such that for $\nu > \nu_2$, $|R(\nu)| < 0.005$ in this particular case.

5.3.2 Sensitivity to Changes in (ν_1, ν_2)

In earlier results we have been looking at the accuracy of the approximate solution for various ranges (ν_1, ν_2) , but how much information from the reflection do we need to be able to get a good idea of the bed topography?

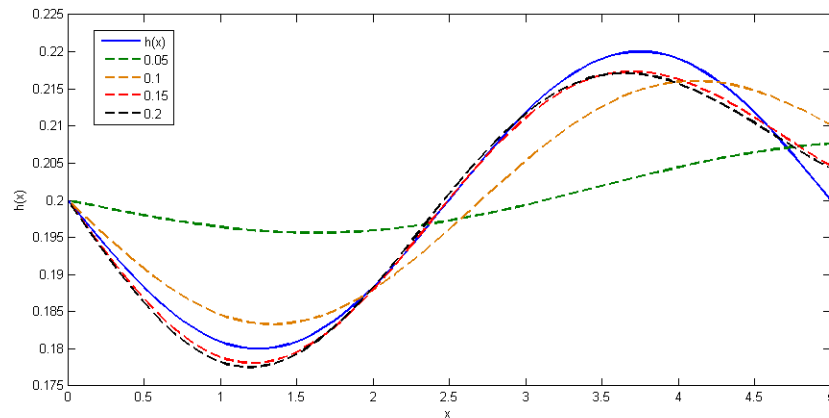


Figure 5.9: Converged depth profiles for $h = h_A$ using the mild-slope approximation, where ν_2 has been allowed to vary.

Firstly, we have kept $\nu_1 = 0.0001$ fixed and allowed ν_2 to vary, but this time for very small values. In Figure 5.9 we can see that as ν_2 is increased, the approximation improves. We can also note that the shape of the approximations, although not very accurate, is close to the desired solution for $\nu \in (0.0001, 0.15)$. This is a very small range and it is rather surprising that the approximation is so good compared to the amount of reflection data that it has to work with.

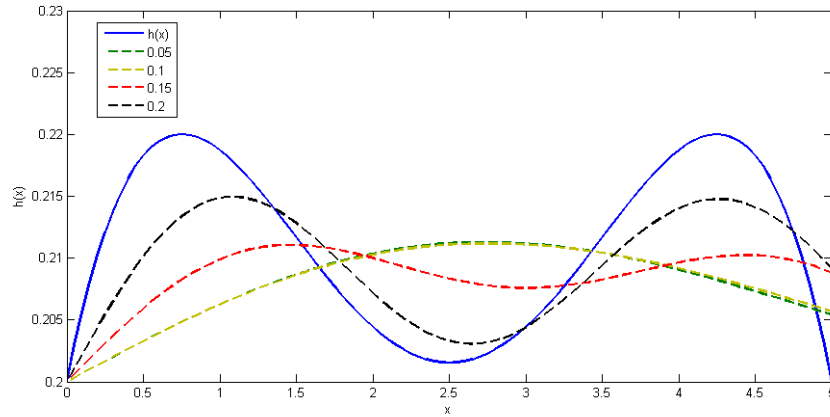


Figure 5.10: Converged depth profiles for $h = h_B$ using the mild-slope approximation, where ν_2 has been allowed to vary.

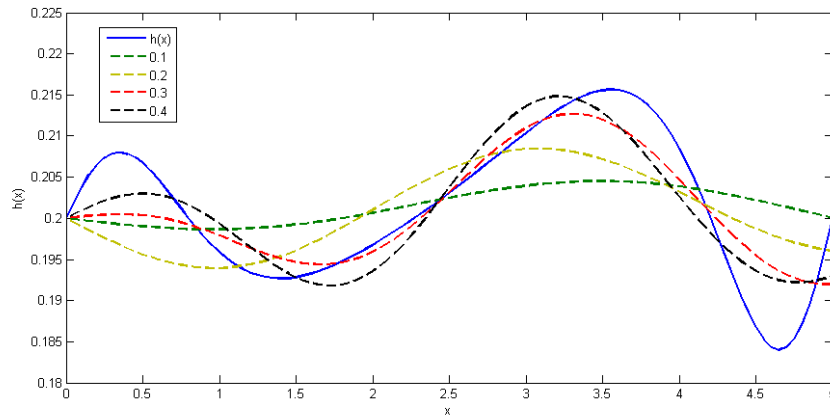


Figure 5.11: Converged depth profiles for $h = h_C$ using the mild-slope approximation, where ν_2 has been allowed to vary.

This level of accuracy for small ν is not shared in each case. For example, in Figure 5.10 with $h = h_B$, we can see that for $\nu \in (0.0001, 0.2)$ the converged solution gives a very crude idea as to the topography, but not yet as accurate as for $h = h_A$. Also for more complicated topographies, as in Figure 5.11 with $h = h_C$, we see that a much larger range for ν is required, since for $\nu \in (0.0001, 0.4)$ the converged solution is only just starting to take the shape of the actual solution.

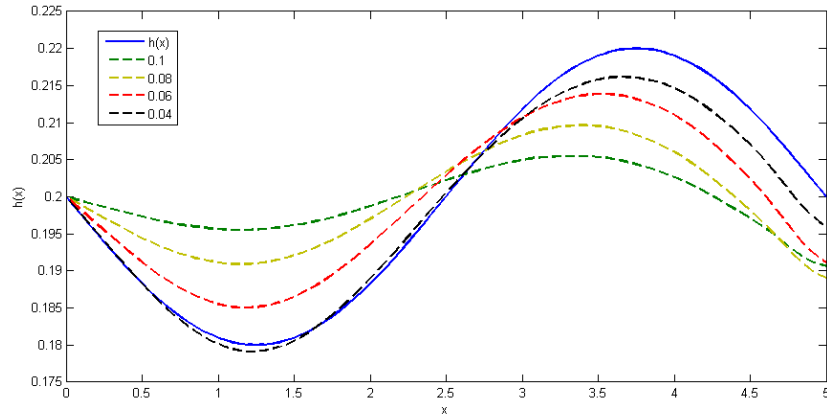


Figure 5.12: Converged depth profiles for $h = h_A$ using the mild-slope approximation, where ν_1 has been allowed to vary.

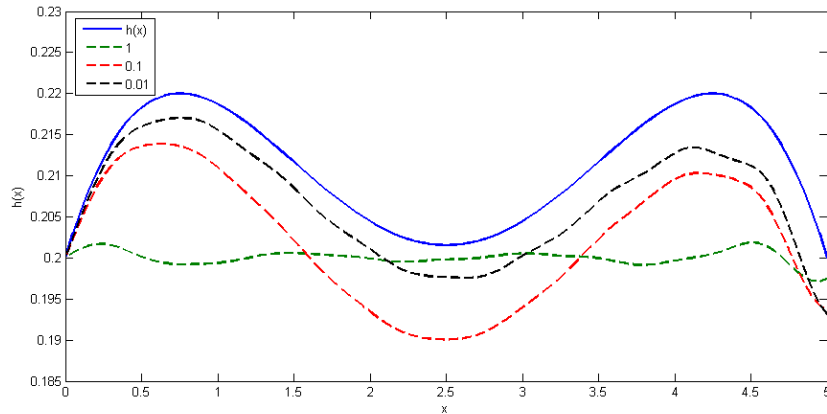


Figure 5.13: Converged depth profiles for $h = h_B$ using the mild-slope approximation, where ν_1 has been allowed to vary.

We are also interested to see how the converged approximation reacts if the smallest values of ν are no longer included. So far we have set $\nu_1 = 0.0001$ and allowed ν_2 to vary, here we shall instead fix $\nu_2 = 5$ and allow ν_1 to vary. From the results we have already gathered, with both ν_1 and ν_2 small, we would expect that increasing ν_1 would only lead to a decrease in accuracy.

From Figures 5.12, 5.13 and 5.14 we can see that this does indeed appear to be the case and furthermore, that for $\nu \in (1, 5)$ the approximations are particularly poor which is an indication that much of the necessary information is in the range $(0, 1)$.

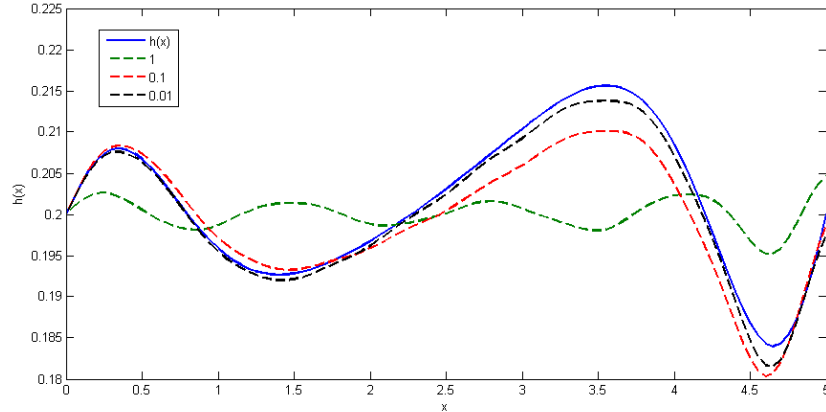


Figure 5.14: Converged depth profiles for $h = h_C$ using the mild-slope approximation, where ν_1 has been allowed to vary.

With this idea that the converged approximations are better for smaller choices of ν_1 , we may wish to consider decreasing it further than just $\nu_1 = 0.0001$.

5.3.3 The Affect of Amplitude

In the convergence results and figures, we have seen that the approximation appears to perform less well at a stationary point in $h(x)$ and that the accuracy of the converged solution could depend on the amplitude of these points. To investigate this possibility we have, without loss of generality, used $h(x) = h_A$ given by

$$h_A(x) = h_a - \epsilon \sin\left(\frac{2\pi x}{l}\right),$$

where $h_a = 0.2$ and $l = 5$. Previously we had set $\epsilon = 0.02$, so that the amplitude of the stationary points was a tenth of the depth, but now we shall allow this to vary.

By making the amplitude of these stationary points larger we expect that the errors will increase, and perhaps that the mild-slope approximation may fail to converge. In Figure 5.15 we can see that with a greater amplitude (half of the depth), the approximation is worse. The first approximation appears to be a fair estimate, but as soon as we begin the iterative process we see that the approximation is wildly inaccurate. Not only have the errors grown substantially but according to the approximation, the bed topography protrudes out of the water's surface.

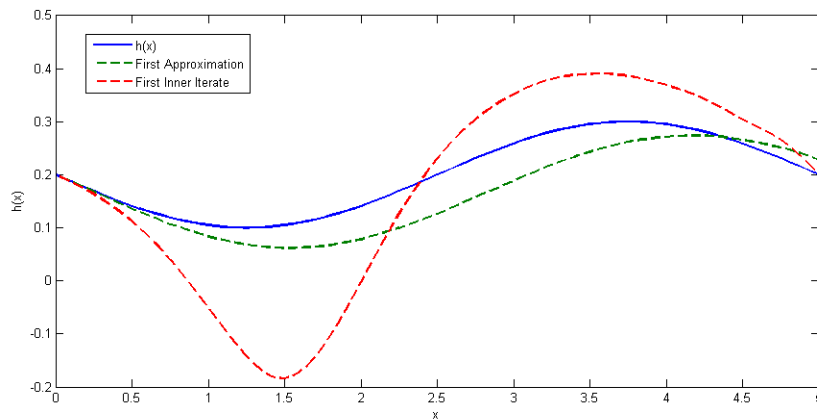


Figure 5.15: Depth profile $h = h_A$ with $\epsilon = 0.1$

Conversely, by making the amplitude of stationary points smaller we get a much more accurate approximation. This is what we would expect since the mild-slope approximation is based on the idea that the gradient is very small and to have a stationary point of lesser amplitude means that the gradient is also less, and so the approximation works better.

Chapter 6

Summary, Future Work & Conclusions

Summary

In some existing literature on linear wave scattering, fundamental ideas of fluid dynamics were used to formulate a boundary value problem for the velocity potential of the water in the (x, z) plane. The solution to this could then be approximated, for simplicity, by using either the shallow water hypothesis that the wavelength is much greater than the quiescent depth, or by using the mild-slope hypothesis that the gradient of the underlying bed topography is small. Reflection and transmission coefficients were also defined for plane waves and had been found to rely on the amplitude of the incident wave. Also, through the use of an identity it was shown that knowing one of these coefficients meant the other could be recovered.

Using this theory and each approximation in turn, we were able to formulate a forward wave scattering problem. We assumed that the bed topography was known along with the amplitude of the incident wave and we were seeking the reflected amplitude, $R(\nu)$ for all $\nu \in (0, \infty)$, where $\nu = \omega^2/g$ (with ω being the frequency of the incident wave, and g the acceleration due to gravity). This turned out to be fairly simple and we were able to find an explicit expression for $R(\nu)$. We then looked at the behaviour of R as $\nu \rightarrow \infty$ and found that for the shallow water approximation R did not tend to zero

as was expected, which may have been due to large ν corresponding to wavelengths smaller than the quiescent depth, going against the shallow water hypothesis. For the mild-slope approximation however, we found that it behaved as we anticipated and decayed exponentially.

We then moved our attention to the more interesting problem of inverse wave scattering, where we were seeking an approximation to the bed topography $h(x)$. We assumed that $R(\nu)$ $\nu \in (0, \infty)$, is known and that the depth at the boundaries of the underlying topography, h_a and h_b , could be measured. The method that we adopted was an iterative one, based on using the approximation $h_n(x)$, to find an improved approximation, $h_{n+1}(x)$, involving inverse Fourier transforms performed on the forward expression found for $R(\nu)$.

It was not clear that this iteration method would produce a convergent sequence, but following tests on the iterations we found that for the mild-slope approximation the iterates began quickly to converge, whereas this was less clear for the shallow water approximation. However, we still had the question of whether the iterates were converging to the solution, $h(x)$. The iterates in the shallow water approximation seemed to perform better for small ν , but compared the mild-slope approximation, they produced wild inaccuracies. For this reason the mild-slope approximation was found to be preferable and so we restricted our attention to it. We then found that the best approximations, $h_n(x)$, were obtained when $R(\nu)$ was known for $\nu \in (\nu_1, \nu_2)$ where $0 < \nu_1 \ll 1$ and ν_2 was large enough and such that for $\nu > \nu_2$ we have $|R(\nu)| < 0.005$. We also found that the curvature of the topography affected the accuracy, where turning points of greater amplitude produced greater errors.

Future Work

In this investigation we have shown numerically that the iteration process for the inverse scattering problem is convergent for the depth profiles tested. This does not mean that the iteration sequence will always converge, and certainly not that they will converge to the desired solution. For this reason we would like to find under what circumstances these iterations converge. Instinct would lead us to believe that this would be dependent

in some way on the norm of the integral operator in (4.9), which in turn is dependent on $h(x)$.

An evident problem with the inverse method is that without prior knowledge of the underlying topography, we have no way of knowing how accurate any given approximation is since the amplitude of the bed profile is not known. A possible solution to this would be to find an approximation, $R_n(\nu)$, to $R(\nu)$ using $h_n(x)$ in (3.11) and examining the error in this approximation. If the error is small it could be reasonable to assume that our approximation $h_n(x)$ is accurate. This leads to the more interesting idea that the reflection $R(\nu)$ is unique to the underlying bed topography.

Another direction for future work is to extend this problem from the one dimensional case, as seen here, to the two dimensional problem where $h = h(x, y)$. Since we have numerical support that suggests the inverse problem in the one dimensional case converges to the bed topography, it is possible that a similar process in two dimensions could also work. This however would require dealing with partial differential equations instead of ordinary differential equations and so the iterative process may become very complicated and computationally expensive.

Conclusions

In the comparison between the shallow water and mild-slope approximations, we have found that although the shallow water approximation is simpler to implement it is too restrictive and so in the inverse case it broke down producing wildly erroneous results. Surprisingly though, the first approximation, $h_1(x)$, using the shallow water approximation gave a good idea of the underlying topography in all tested cases. Therefore if only a rough estimate of the topography is required we may simply find the first approximation, $h_1(x)$, using (4.5).

In contrast, the mild-slope approximation delivered very accurate results for the inverse scattering problem and moreover, we have been able to show that even with very small ranges of ν , accurate approximations can be attained. This implies that for better numerical computation, we can take a smaller range of ν and use a finer mesh on it, rather than a coarser mesh on a larger range of ν . This idea is supported by the

results in Section 5.3.1, since we have also seen that including larger values of ν may not increase accuracy and so may be neglected. The accuracy of the approximation however, is also dependent on the amplitude of any stationary points in the bed profile, $h(x)$. The smaller the amplitude, the greater the accuracy meaning that to know our results are accurate we must already know that the gradient of the bed profile is very mild.

Therefore with a small range of reflected data, $R(\nu)$, and some prior knowledge that the bed profile is mild, we can use the iterative inverse method and mild-slope approximation to find an accurate representation of the underlying topography.

Bibliography

- [1] PORTER, D. & CHAMBERLAIN, P. G.: Linear wave scattering by two-dimensional topography *In Gravity waves on water of finite depth* (ed. J.N. Hunt). **Computational Mechanics**, 1997, 13–53.
- [2] CHAMBERLAIN, P. G.: Wave scattering over uneven depth using the mild-slope equation. *Wave Motion*, **17**, 1993, 267–285
- [3] PORTER, D.: The Mild-Slope Equations, *J. Fluid Mechanics*, **494**, 2003, 51–63.
- [4] HACKBUSCH, W.: *Integral Equations, Theory and Numerical Treatment*, Birkhäuser, 1995
- [5] DAVIES, B.: *Integral Transforms and Their Applications - Third Edition*, Springer, 2002
- [6] LANDAU, L. D. & LIFSHITZ, E. M.: *Fluid Mechanics - Second Edition*, Elsevier, 2004
- [7] THE MATHWORKS: *Using MATLAB Version 6*, The MathWorks Inc., 2000
- [8] www.wikiwaves.org, Wikipedia exclusively for Waves, (checked on 05.07.2008)
- [9] www.mathworld.wolfram.com, MathWorld: online mathematics resource, (checked on 02.08.2008)

Appendix A

More Tables And Figures

A.1 Shallow Water Approximation

Inner Iteration Convergence

Following on from the results for the inner iteration convergence in Section 5.2.1, Tables A.1, A.2 and A.3 show the error between iterations for a larger range of $\nu \in (\nu_1, \nu_2)$. These results do not imply convergence to the solution.

	$\ h_2^{(m)} - h_2^{(m-1)}\ _\infty$		
m	h_A	h_B	h_C
2	0.0678	1.8175	0.3929
3	0.1135	9.0984	0.3124
4	10.9085	68.3473	0.2286
5	27.8077	68.1714	0.1371
10	0.731	0.0186	0.2667
15	0.0015	3.67×10^{-4}	0.1513

Table A.1: Maximum error between the $(m)^{th}$ and $(m-1)^{th}$ iterate with $\nu_2 = 5$, using the shallow water approximation.

	$\ h_2^{(m)} - h_2^{(m-1)}\ _\infty$		
m	h_A	h_B	h_C
2	6.9635	84.6378	10.7729
3	8.9364	6.7553	10.5104
4	9.1073	0.7272	18.9734
5	1.4282	0.1739	19.2164
10	1.78×10^{-5}	9.26×10^{-8}	0.8124
15	1.38×10^{-9}	6.92×10^{-12}	2.70×10^{-4}

Table A.2: Maximum error between the $(m)^{th}$ and $(m - 1)^{th}$ iterate with $\nu_2 = 10$, using the shallow water approximation.

	$\ h_2^{(m)} - h_2^{(m-1)}\ _\infty$		
m	h_A	h_B	h_C
2	93.2334	13.445	6.4016
3	92.9916	4.1052	22.7819
4	1.1235	1.0531	22.8502
5	0.0614	0.0103	0.6481
10	5.62×10^{-8}	7.87×10^{-9}	1.46×10^{-4}
15	1.66×10^{-14}	6.56×10^{-15}	9.97×10^{-8}

Table A.3: Maximum error between the $(m)^{th}$ and $(m - 1)^{th}$ iterate with $\nu_2 = 15$, using the shallow water approximation.

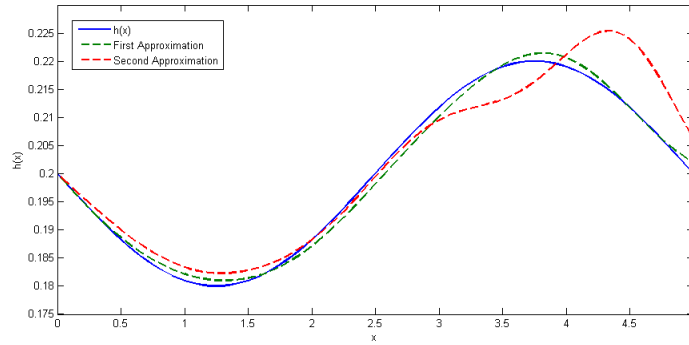


Figure A.1: Comparison of h_1 with h_2 using $h = h_A$ and $\nu_2 = 1$.

The results from Table 5.4 implied that for $\nu \in (0.0001, 1)$ the inner iteration process converged to h_2 . Figure 5.4 shows this converged limit for $h = h_B$, and in Figures A.1

and A.2 are the converged limits for $h = h_A$ and $h = h_B$ respectively. It is also clear from these figures that the second iterate is not converging to the solution $h(t)$.

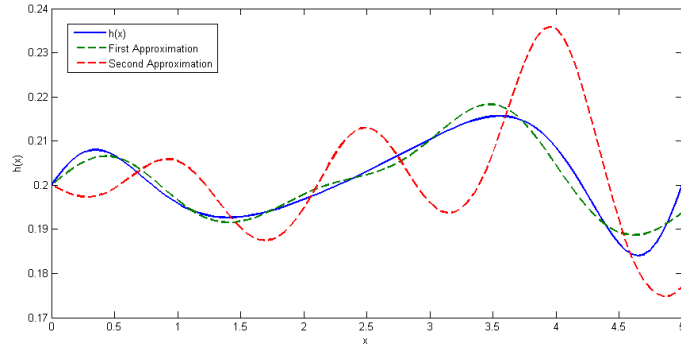


Figure A.2: Comparison of h_1 with h_2 using $h = h_C$ and $\nu_2 = 1$.

Outer Iteration Convergence

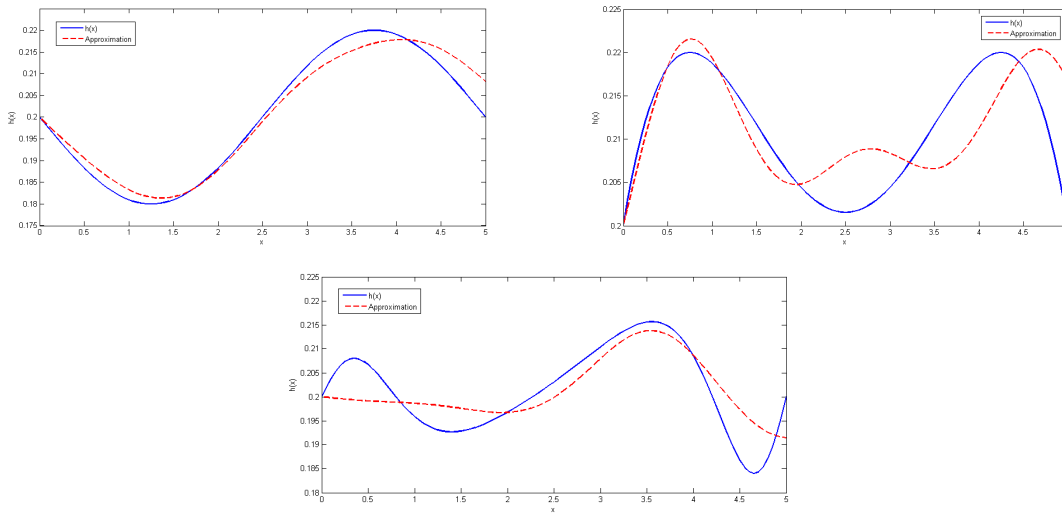


Figure A.3: Converged depth profiles for h_A , h_B and h_C respectively with $\nu_2 = 0.5$, using the shallow water approximation.

Once inner iteration convergence was established we moved on to the outer iteration convergence for the shallow water approximation, and concentrated on small values for ν_2 . Following on from the results given in Section 5.2.2, Figures A.3 and A.4 show the converged approximations to $h(x)$ for other ranges of ν .

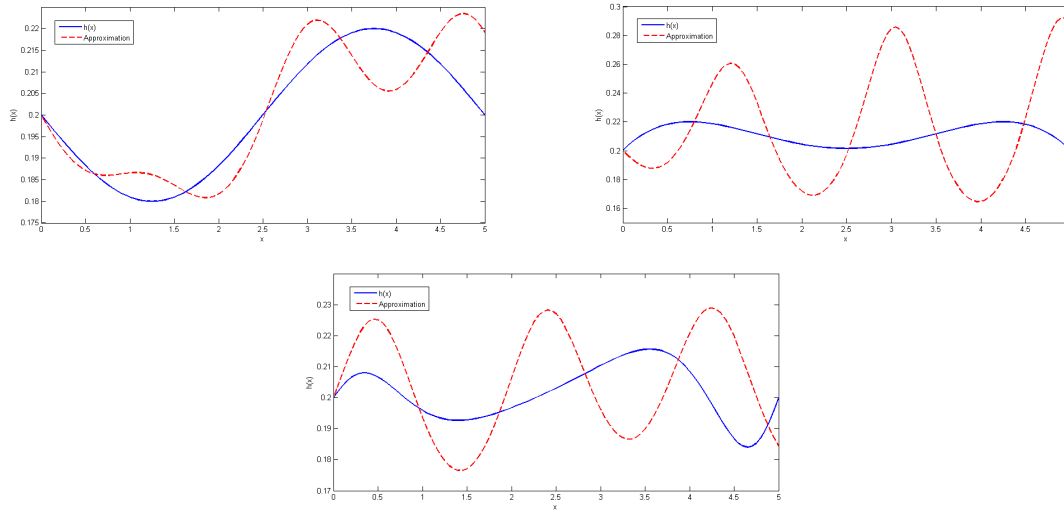


Figure A.4: Converged depth profiles for h_A , h_B and h_C respectively with $nu_2 = 0.7$, using the shallow water approximation.

A.2 Mild-Slope Approximation

Inner Iteration Convergence

Following on from the results for the inner iteration convergence in Section 5.2.2, Tables A.4 and A.5 show the error between iterations for different ranges of $\nu \in (\nu_1, \nu_2)$. These results help to reinforce the implication that inner iterations are converging using the mild-slope approximation. As was noted in Section 5.2.2 the convergence for the mild-

m	$\ h_2^{(m)} - h_2^{(m-1)}\ _\infty$		
	h_A	h_B	h_C
2	2.43×10^{-4}	6.50×10^{-4}	1.14×10^{-4}
3	2.97×10^{-5}	2.00×10^{-4}	9.00×10^{-6}
4	5.39×10^{-6}	4.41×10^{-5}	7.98×10^{-7}
5	8.77×10^{-7}	1.31×10^{-5}	6.69×10^{-8}
10	8.81×10^{-10}	1.86×10^{-8}	2.91×10^{-13}
15	1.93×10^{-12}	3.24×10^{-11}	2.78×10^{-17}

Table A.4: Maximum error between the $(m)^{th}$ and $(m-1)^{th}$ iterate with $\nu_2 = 5$, using the mild-slope approximation.

m	$\ h_2^{(m)} - h_2^{(m-1)}\ _\infty$		
	h_A	h_B	h_C
2	2.68×10^{-4}	7.39×10^{-4}	1.13×10^{-4}
3	3.34×10^{-5}	1.39×10^{-4}	7.79×10^{-6}
4	6.21×10^{-6}	4.01×10^{-5}	7.95×10^{-7}
5	1.12×10^{-6}	5.07×10^{-6}	6.53×10^{-8}
10	1.19×10^{-9}	1.05×10^{-8}	6.00×10^{-13}
15	4.26×10^{-12}	1.16×10^{-11}	2.78×10^{-17}

Table A.5: Maximum error between the $(m)^{th}$ and $(m-1)^{th}$ iterate with $\nu_2 = 15$, using the mild-slope approximation.

slope approximation appears to faster than for the shallow water approximation. This is quite evident by comparing Tables A.4 and A.5 with Tables A.1, A.2 and A.3 as the errors for the mild-slope approximation are smaller and decrease faster as m is increased.

It is also evident, by simply comparing Figures A.5 and A.6 with Figures A.1 and A.2, that the mild-slope approximation produces far more accurate second iterates, $h_2(x)$,

than the shallow water approximation.

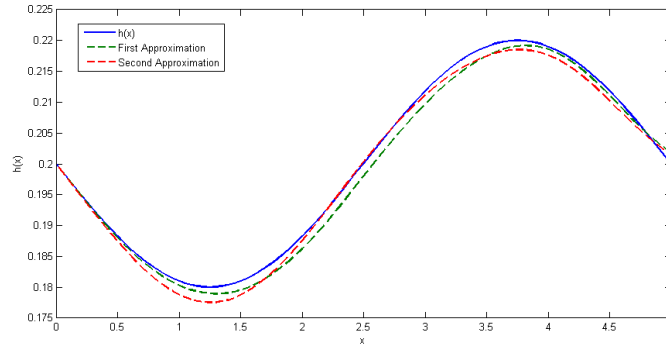


Figure A.5: Comparison of h_1 with h_2 using $h = h_A$ and $\nu_2 = 1$.

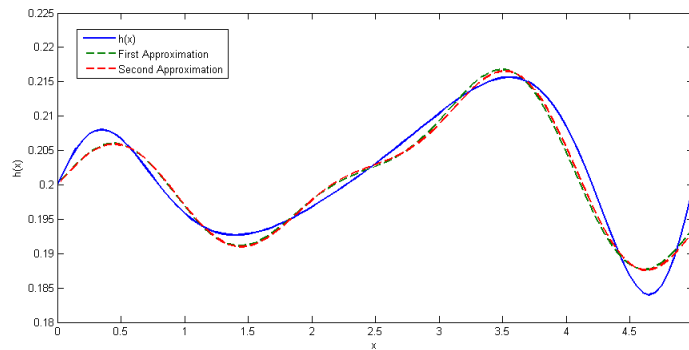


Figure A.6: Comparison of h_1 with h_2 using $h = h_C$ and $\nu_2 = 1$.

Outer Iteration Convergence

We have already seen that the inner iteration process is more accurate for the mild-slope approximation and so, as we may expect, is the outer iteration process. This has been shown by looking at errors in Section 5.2.2 but is very clear to see by comparing Figures A.7 and A.8 with Figures A.3 and A.4.

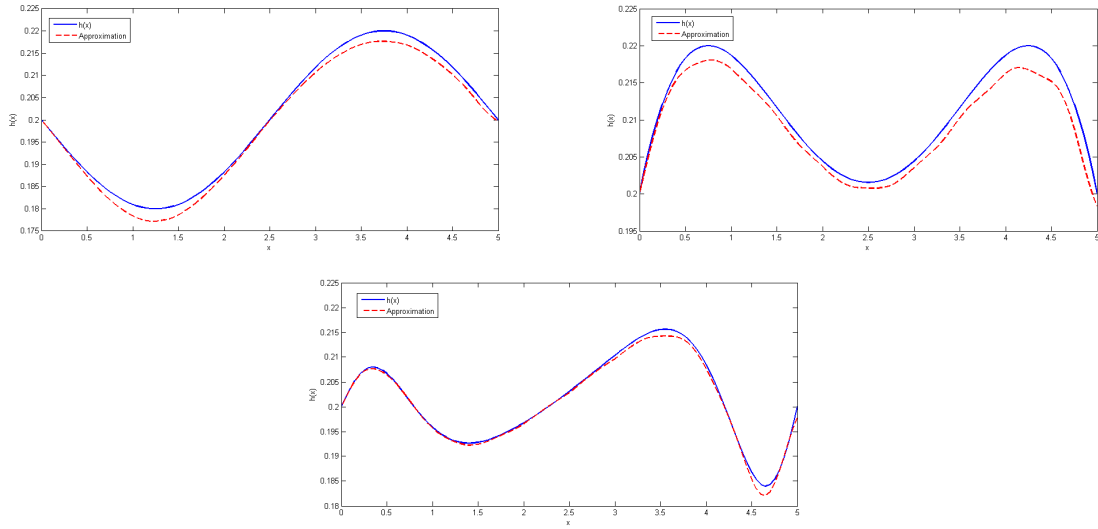


Figure A.7: Converged depth profiles for h_A , h_B and h_C respectively with $\nu_2 = 5$, using the mild-slope approximation.

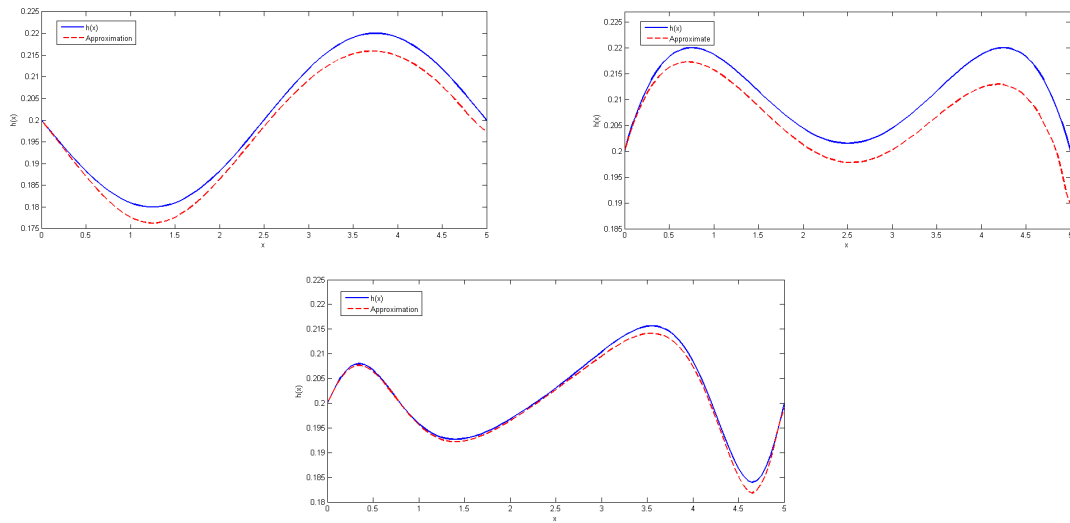


Figure A.8: Converged depth profiles for h_A , h_B and h_C respectively with $\nu_2 = 15$, using the mild-slope approximation.